ISSN 2223-3911

INDUSTRIAL TECHNOLOGY AND ENGINEERING

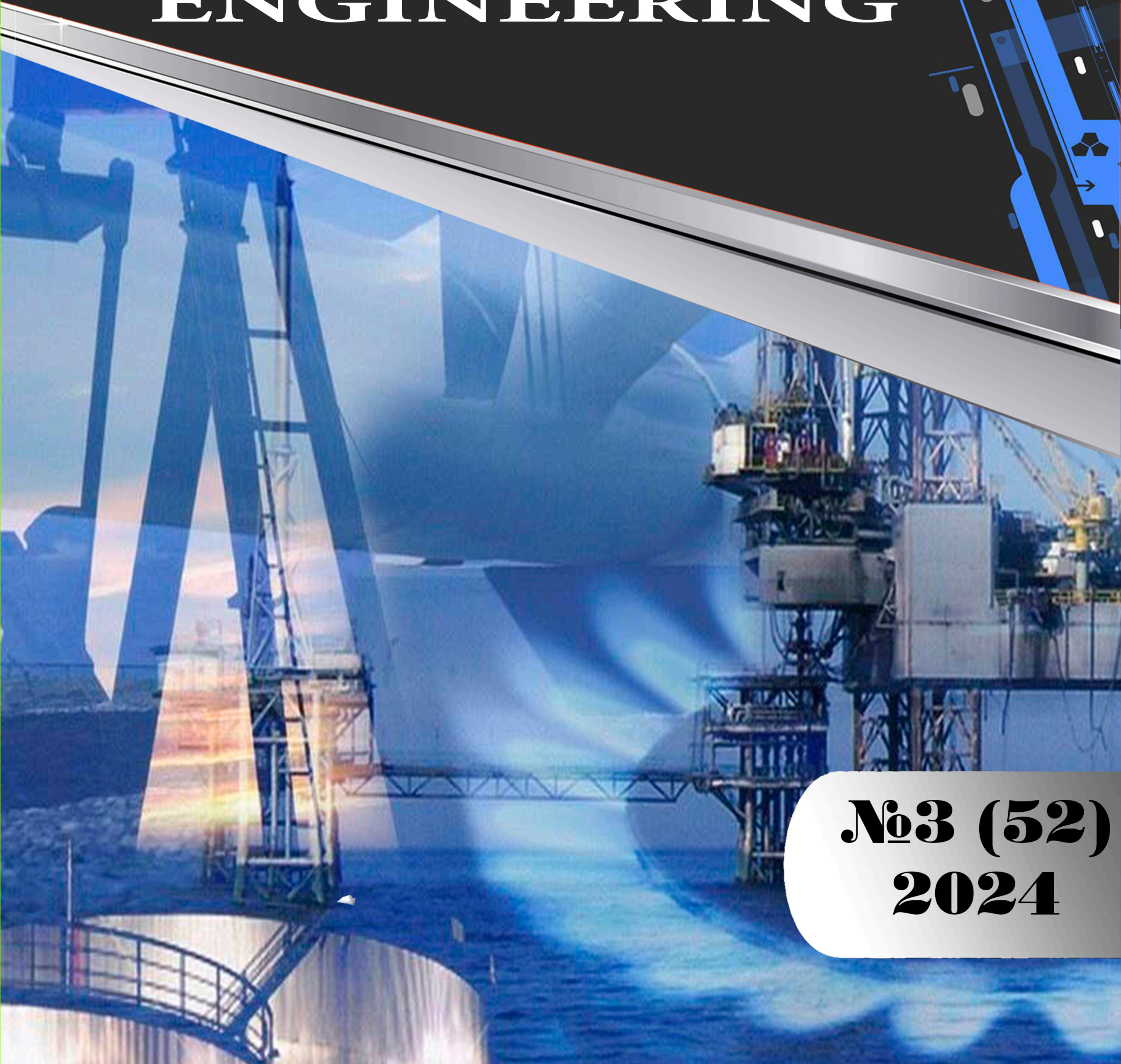

№3 (52)
2024

ISSN 2223-3911

Industrial Technology
and
Engineering

№ 3 (52) 2024

The journal is being published since 2011, Periodicity: 4 issues per year

Editor in chief: *A. Bayeshov*

The Owner: Ministry of Education and Science of the Republic of Kazakhstan
Non-Profit Joint Stock Company «M. Auezov South Kazakhstan University»

Certificate of registration of the periodic printed publication and (or) news agency № 11566-Ж issued on 04.04.2011 by Ministry of Communication and Information of the Republic of Kazakhstan.
The journal is registered at the International Centre for Registration of serial editions (UNESCO, Paris, France) in June 2011 under registration number ISSN 2223-3911.

Address:
Tauke khan avenue, 5
160012 Shymkent, Kazakhstan
Phone/Fax: +7 (7252) 21-19-82/21-19-89.
E-mail: ite_sksu@mail.ru

Printed in Kazakhstan

EDITORIAL BOARD

EDITOR –IN-CHIEF

Abduali Bayeshov – Dr.Chem.Sc., Professor, Academician of National Academy of Science of the Republic of Kazakhstan, Almaty, Kazakhstan. (39/4)

DEPUTIES OF EDITOR –IN-CHIEF

Mohamad Nasir Mohamad Ibrahim – PhD, Associate Professor, Universiti Sains Malaysia, Penang, Malaysia. (176/38)

Izabella Nowak – Dr., Professor, Adam Mickiewicz University in Poznan, Poznan, Poland. (153/30)

EDITORIAL BOARD

Jamal Khatib – Dr., Professor, University of Wulverhampton, Wulverhampton, the United Kingdom. (173/32)

Polina Prokopovich – PhD, Cardiff University, Cardiff, the United Kingdom. (93/27)

Boguslawa Leska – PhD, Professor, Adam Mickiewicz University in Poznan, Poznan, Poland. (96/19)

Aleksandr Kolesnikov – Cand.Tech.Sci., Associate Professor, M. Auezov South Kazakhstan University, Shymkent, Kazakhstan. (47/17)

Vyacheslav Naraev – Dr.Chem.Sc., Professor, Saint Petersburg State Institute of Technology (Technical University), Saint Petersburg, Russia. (27/10)

Oralgazy Nurkenov – Dr.Chem.Sci., Professor, Institute of Organic Synthesis and Coal Chemistry of Republic of Kazakhstanб National Academy of Science of Kazakhstan (117/7)

Serik Fazylov - Dr.Chem.Sci., Professor, Buketov Karaganda University, Karaganda, Academician of National Academy of Science of the Republic of Kazakhstan, Almaty, Kazakhstan. (101/7)

Kazim Nadirov – Dr.Chem.Sc., Professor, M. Auezov South Kazakhstan University, Shymkent, Kazakhstan. (22/7)
Saule Akhmetova – Cand.Tech.Sci., Associate Professor, Almaty Technological University, Almaty, Kazakhstan. (29/6)

Svetlana Yefremova – Dr.Tech.Sci., Professor, National Center on Complex Processing of Mineral Raw Materials of the Republic of Kazakhstan, Almaty, Kazakhstan (17/6)

Irina Pochitalkina – Dr.Tech.Sc., Professor, D.I. Mendeleyev Russian Chemical and Technological University, Moscow, Russia. (31/5)

Malik Satayev – Dr.Tech.Sc., Professor, M. Auezov South Kazakhstan University, Shymkent, Kazakhstan. (24/5)

Sergey Kalugin – Dr.Chem.Sci., Professor, Al Farabi Kazakh National University, Almaty, Kazakhstan (18/5)

Sarsenbek Turtabayev – Dr.Tech.Sci., Professor, Khoja Akhmet Yassawi International Kazakh-Turkish University, Turkistan, Kazakhstan (14/5)

Ulzhalgas Nazarbek – PhD Associate Professor, M. Auezov South Kazakhstan University, Shymkent, Kazakhstan. (25/4)

Umirzak Dzhusipbekov - Dr.Chem.Sci., Professor, Institute of Chemical Sciences named after A.B. Bekturov, Corresponding member of National Academy of Science of the Republic of Kazakhstan, Almaty, Kazakhstan. (9/3)

Gulnora Ikhtiyarova - Dr.Chem.Sci., Professor, Tashkent State Technical University, Tashkent, Uzbekistan

IRSTI 61.13.17

FEATURES OF MODELING THERMAL PROCESSES IN A SHALLOW BOREHOLE HEAT EXCHANGER

Altynbekov R.F.[1*], Matsevity Yu.M.[2], Kostikov A.O.[2], Saipov A.A.[1], Duisengali G.B.[1]
[1]*M. Auezov South Kazakhstan University, Shymkent, Kazakhstan*
[2]*Anatolii Pidhornyi Institute of Power Machines and Systems of the National Academy of Sciences of Ukraine, Kharkiv, Ukraine*
***Corresponding Author’s Email: rustik2030@inbox.ru**

ABSTRACT

The article considers the features of modeling thermal processes in shallow borehole heat exchangers, which are widely used in geothermal heating and cooling systems. The main attention is paid to the factors affecting the efficiency of heat exchange between the heat carrier and the ground, including soil thermal conductivity, the presence of groundwater, seasonal temperature variations and heat flux density. The authors describe numerical modeling methods suitable for analyzing heat exchange in a porous medium and consider the application of the finite element method to improve the accuracy of calculations. A study was conducted of the influence of such parameters as borehole depth, distance between boreholes and heat exchanger configuration on the temperature distribution in the surrounding rock. The presented modeling results demonstrate changes in the thermal characteristics of the system depending on various climatic and geological conditions, which allows optimizing the design of borehole heat exchangers in dense urban areas. The findings may be useful for engineers and designers involved in the development and implementation of geothermal systems, as well as for further research in the field of modeling thermal processes in ground heat exchangers.

Keywords: borehole heat exchanger, thermal processes, shallow occurrence, modeling, geothermal heating, heat exchange, heat transfer, groundwater, thermal conductivity, numerical modeling.

INTRODUCTION

Modeling thermal processes in a shallow borehole heat exchanger requires taking into account a number of specific factors and conditions associated with its features. Key features of such systems:

1. Heat transfer in the ground

- Borehole heat exchangers operate by transferring heat between the coolant (usually liquid) in the pipeline and the surrounding ground environment. The ground acts as a heat accumulator, accepting or giving off heat depending on the season.

- When modeling, it is important to take into account the thermal conductivity of the soil, its moisture content, porosity and density [1-3]. All these parameters have a significant impact on the efficiency of the system, especially in the long term.

2. Borehole geometry and heat exchange tube arrangement

- Typically, shallow borehole heat exchangers use tubes that form a “double U-shape” or “coaxial” circuit. Geometric parameters such as borehole depth, diameter, and spacing affect the heat transfer rate.

- The arrangement of boreholes relative to each other is also important [4-6]. If boreholes are too close, thermal interactions may occur between them, which reduces the overall efficiency of the system.

3. Heat carrier dynamics

- A heat carrier (water or antifreeze) circulates in the heat exchange pipes, absorbing heat from the ground in winter and releasing it in summer. The speed and temperature of the heat carrier change depending on the operating mode and ground temperature, which must be taken into account in the model.

- Heat carrier parameters such as its heat capacity, viscosity and thermal conductivity affect the thermal power of the system [7-9].

4. Seasonal changes in soil temperature

- Soil temperature at shallow depths (usually up to 30-50 meters) is subject to seasonal fluctuations. For modeling, it is necessary to take into account seasonal changes in air temperature, which can affect the upper soil layers and, therefore, the efficiency of the system.

- In addition, with increasing operating time, the system can lead to a gradual change in soil temperature, which requires taking into account long-term thermal effects [10,11].

5. Heat exchanger operating mode

- Borehole heat exchangers can operate in intermittent or continuous mode. Continuous operation of the system can lead to “freezing” of the soil in winter or its overheating in summer if appropriate control measures are not provided.

- For more accurate modeling, it is important to consider how the heat consumption from the building and the operating characteristics of the system (e.g. interruptions in operation) will change.

6. Thermal inertia of the system

- The soil has significant thermal inertia and its temperature changes slowly under the influence of the heat exchanger. This means that borehole heat exchangers are particularly effective at providing a constant level of heat, but their efficiency decreases with sudden changes in load.

7. Boundary conditions and numerical methods

- Numerical methods such as finite differences or finite elements are often used to accurately model thermal processes. It is important to set the boundary conditions correctly: the soil temperature at the initial stage, the conditions on the surface, and the properties of the heat carrier.

- Sometimes combined modeling is used using geothermal and hydrodynamic models, which allows for the interaction of the heat carrier with the soil to be taken into account more accurately [9-14].

Modeling thermal processes in shallow borehole heat exchangers requires taking into account many factors: soil thermal conductivity, heat carrier dynamics, seasonal temperature fluctuations, and borehole geometry. Correct modeling allows to evaluate the efficiency of the system and prevent problems such as freezing or overheating of the soil.

Thus, geometric inverse heat exchange problems play a key role in determining parameters that are not directly measurable using temperature and heat flux data.

When developing a heat supply system (including those based on borehole heat exchangers), it is necessary to conduct thorough studies to find the optimal design and operating parameters. Since experimental studies are very expensive and cannot provide all the necessary information, the most effective tool is mathematical modeling and identification of thermal processes. Note that in the modeling process, it is necessary to take into account the mutual thermal influence in the “rock – borehole heat exchangers” system (deep heat heats the heat carrier, which, in turn, cools the rock mass located directly near the borehole).

The mathematical model of the thermophysical processes occurring during the extraction of petrothermal heat includes a non-stationary heat conduction equation describing the thermal process in a rock massif (it is assumed that its temperature field has axial symmetry relative to the borehole),

$$c\rho\frac{\partial T}{\partial \tau}=\frac{1}{r}\frac{\partial}{\partial r}\left(\lambda r\frac{\partial T}{\partial r}\right)+\frac{\partial}{\partial z}\left(\lambda\frac{\partial T}{\partial z}\right) \tag{1}$$

and equations describing the heat exchange of the heat carrier with the section of rock adjacent to the borehole:

$$\begin{aligned} &w_1\rho_{\mathrm{HC}}c_p r_1\frac{\partial T_1}{\partial z}=2k_1\left(T_1(\tau,z)-T_2(\tau,z)\right),\\ &w_2\rho_{\mathrm{HC}}c_p\left(r_3^2-r_2^2\right)\frac{\partial T_2}{\partial z}=2r_3\alpha_3^E\left(T(\tau,r_4,z)-T_2(\tau,z)\right)+2r_2k_2\left(T_2(\tau,z)-T_1(\tau,z)\right).\end{aligned} \tag{2}$$

The latter are written under the assumption that due to the sufficiently high speed of the heat carrier movement, heat transfer along the borehole axis due to thermal conductivity in the heat carrier can be neglected. For the same reason, the thermal process in the heat carrier can be assumed to be quasi-stationary (therefore, non-stationary terms are omitted in expressions (2). Also, when writing (2), the assumption is made that the heat carrier temperature in the cross-section of the pipe does not depend on the coordinates.

On the outer surface of the production string, the boundary condition is set:

$$\lambda\left.\frac{\partial T}{\partial r}\right|_{r_4}=\alpha_3^{\mathrm{E}}\left(T(\tau,r_4,z)-T_2(\tau,z)\right) \tag{3}$$

In expressions (1)–(3) τ – time; r, z – radial and axial coordinates; $T = T(\tau, r, z)$ – the rock mass temperature; c – the specific heat capacity of the rock; ρ – its density; λ – its thermal conductivity; w_1 and w_2 – the speed of the heat carrier rising in the inner pipe and descending in the annular space, respectively; ρ_{HC} and c_p – the density and specific heat capacity of the heat carrier at constant pressure; T_1 and T_2 – the temperature of the heat carrier rising in the inner pipe and descending in the annular space, respectively; r_1 – the inner radius of the lift string; r_2 – is the outer radius of the intermediate string; r_3 and r_4 – the inner and outer radii of the production string; α_3^E – the equivalent (taking into account the thermal resistance of the wall of the production string) heat transfer coefficient on its inner surface; k – the heat transfer coefficients through the lift and intermediate columns and the air gap between them, indices 1 and 2 at the coefficient k indicate that it is related to the inner surface of the lift string or to the outer surface of the intermediate string, respectively. Since all three heat transfer mechanisms take part in the air gap between the pipe strings, both the convective and radiant components must be taken into account in the coefficient k.

The initial conditions are the temperature distribution in the rock massif without the thermal influence of borehole heat exchangers. Since the borehole depth is orders of magnitude greater than the depth of the neutral layer, above which daily and annual temperature variations are observed, this small section of soil can be neglected and boundary conditions of the I kind can be set on the upper part of the rock massif considered in the problem with a temperature equal to the constant temperature of the neutral layer, which, as noted above, corresponds to the average annual temperature for this region. Boundary conditions of the I kind are also accepted on the remaining surfaces of the rock massif, the temperature in which is set based on the change in the temperature of the rock with depth, not subject to the influence of borehole heat exchangers. Obviously, this can be done only if equation (1) is considered in a rock massif of such dimensions that the thermal influence of borehole heat exchanger does not reach its outer boundaries.

The boundary of the borehole heat exchanger influence zone on the rock can be determined by solving the geometric inverse heat exchange problem. In order to minimize the number of identifiable geometric parameters and, thereby, speed up the process of solving the inverse heat exchange problem, it is advisable to consider a cylindrical rock massif that contains the borehole heat exchanger influence zone, with the dimensions of this cylinder (height z_M and radius r_M) being minimal (Fig. 1). Obviously, if the calculation area is smaller than the above-mentioned cylinder, this will lead to distortion of the initial data at its boundary, and, consequently, to distortion of the solution results. If the calculation area is made larger without changing the step of the difference grid, this will not affect the accuracy of the solution, but will lead to the fact that the number of grid nodes, and, consequently, the calculation time will increase. In numerical modeling, the z_M and r_M values were determined based on the condition that the temperature at each point of the boundary of a cylindrical rock mass deviates from the undisturbed temperature of the rock for a given depth by no more than 0.01°C.

Note that this mathematical model is nonlinear due to the fact that the thermophysical properties of the rock and the heat carrier depend on their temperatures.

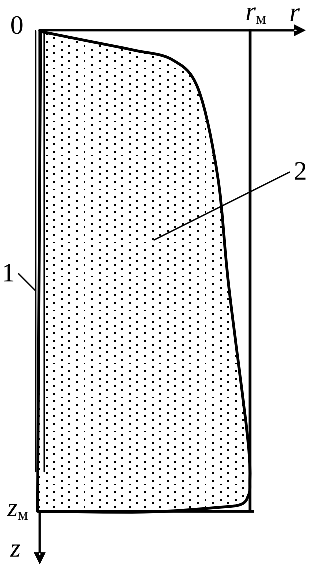

Fig. 1. The computational domain in the problem of modeling thermal processes during the extraction of petrothermal energy: 1 – borehole; 2 – zone of influence of the borehole heat exchanger

MATERIALS AND METHODS

To perform the calculations, a program was created in which the problem of thermal conductivity in a rock mass was solved using the difference method, and an iterative process was used to take into account the influence of equations (2) on the boundary conditions (3). A typical well was considered, the parameters of which are typical for gas wells of Kharkiv gazdobycha Gas Production Department, located in Kharkiv region: depth 5000 m, production string 140x10.5, borehole bottom temperature 130°C, neutral layer temperature 7.8°C. The lift string is organized from 48x4.0 tubing pipes, and the intermediate one is 89x6.5. The thermophysical properties of the soil were taken to be c = 1040 J/(kg·K), ρ = 2800 kg/m^3, λ = 2.6 W/(m·K), the mass flow rate of the heat carrier was 1.75 kg/s, and its temperature at the inlet to the borehole heat exchanger was 20°C.

RESULTS AND DISCUSSION

It should be noted that from the point of view of thermal physics, the soil is a rather complex system. Firstly, it consists of a skeleton, including many small solid particles of various shapes, sizes and natures. Secondly, the pores of this skeleton are filled with a mobile medium (usually humid air and mineralized water), which, depending on the temperature, can change its aggregate state. Thirdly, under the action of capillary, gravitational forces, and also as result of the flow of underground groundwater, movement of this medium relative to the soil can occur, which can also involve individual particles of the skeleton.

A detailed description of all these factors in a mathematical model is quite difficult. However, taking into account that the sizes of the skeleton grains and pores are insignificant compared to the geometric characteristics of the ground heat exchanger, the soil can be considered as a homogeneous solid with averaged thermophysical properties [8], which integrally take into account these physical phenomena. This approach proved itself in practice for the design and calculation studies of ground heat exchangers [5, 12, 14].

The formation of the thermal regime of the soil massif in which the borehole is located occurs under the influence of three factors: weather and climate conditions (air temperature, wind, precipitation, solar radiation), heat flow from the entrails of the earth and thermal impact from the ground heat exchanger. The soil of the surface layers of the earth is subject to clearly expressed seasonal and daily temperature fluctuations as a result of changes in the outside air temperature and the intensity of solar radiation. Therefore, as boundary conditions on the boundary of the soil massif in question, which coincides with the earth’s surface, it is necessary to set not boundary conditions of the I kind, as was done above when modeling the borehole heat exchanger, but a combination of boundary conditions of the II and III kind

$$\lambda \left.\frac{\partial T}{\partial z}\right|_{z=0} = \alpha_{\mathrm{es}} \left(T\big|_{z=0} - T_{\mathrm{a}} \right) + q_{\mathrm{rad}} , \tag{4}$$

where $\alpha_{\text{пз}}$ – the heat transfer coefficient on the earth’s surface; $T_{\text{а}}$ – the atmospheric air temperature; $q_{\text{л}}$ – the radiant heat flow on the earth’s surface, determined by the difference between the absorbed solar radiation and the radiation from the earth’s surface.

It should be noted that equation (4) does not take into account heat exchange on the earth’s surface due to moisture evaporation and precipitation. These thermal processes are quite complex and heavily dependent on weather conditions, which, when describing them in detail, would require the use of a stochastic approach when compiling a mathematical model. The values $\alpha_{\text{пз}}$, $T_{\text{а}}$ and $q_{\text{л}}$ also depend on weather conditions. Thus, in cloudy weather, direct solar radiation, i.e., electromagnetic radiation absorbed by the earth’s surface, emanating directly from the sun, is absent and the only radiant source of heat is the part of the solar radiation that has been scattered in the atmosphere. In order to avoid taking into account all of the above factors that affect heat exchange on the earth’s surface, it seems rational to use the averaged values $\alpha_{\text{пз}}$, $T_{\text{а}}$ and $q_{\text{л}}$, which results in their having a cyclical dependence (both daily and annual) on time. In some cases, the daily cyclicity can be neglected.

On the remaining parts of the boundary of the soil massif, as in the case of a borehole heat exchanger, boundary conditions of the first kind are specified, corresponding to the temperature of the soil massif not subject to the thermal influence of the ground heat exchanger. The only difference here is that the temperature specified on the boundary is a function of not one variable z, but two – a dependence on time is added, caused by daily and annual fluctuations. This dependence can be constructed as a result of approximation of experimental data or by analytical methods. For example, under the assumption that the thermophysical properties of the soil do not depend on its temperature, and daily fluctuations can be neglected, the temperature of the soil not subject to the thermal influence of the ground heat exchanger is described by expression (5)

$$T(z,\tau) = Ae^{-\sqrt{\frac{\omega}{2a}}z}\cos\left(\sqrt{\frac{\omega}{2a}}z - \omega\tau\right) + T_c\,, \qquad (5)$$

where A and ω – the amplitude and frequency of the soil surface temperature fluctuations; T_c – the average annual temperature on the soil surface.

Another difference in the mathematical models of a borehole heat exchanger and a ground heat exchanger is the modeling of the wall separating the descending and ascending flows of the heat carrier. In the case of shallow boreholes, rubber hoses or polypropylene pipes are lowered into the boring casing to organize the counterflow of the heat carrier. Since in this case there is no air annular gap, there is a homogeneous medium (the wall of the pipe lowered into the borehole) between the radii r_1 and r_2 (see Fig. 1). Thus, when calculating the heat transfer coefficient k, which appears in expressions (2), there is no need to take into account the convective and radiant components.

As in the case of borehole heat exchanger, to determine the zone of thermal influence of the ground heat exchanger on the soil massif, it is necessary to use the tools of the geometric inverse heat exchange problem. The configuration of the calculation area and the identified geometric parameters remain the same (see Fig. 1).

CONCLUSION

The considered technology of petrothermal energy extraction can be used in technological processes at the field itself, where the well is located, or for heating and hot water supply of industrial buildings of the field. It is also possible to transfer the heat carrier to populated areas, greenhouses, etc., which are located at a short distance (up to 2-3 km) from the well. In each case, after specifying the initial data, it is necessary to conduct additional calculation studies to select effective design and operating parameters, taking into account the number and depth of existing wells, their distance from the consumer, types of rocks, type of consumer and other factors.

The calculations carried out allowed to conclude that in order to obtain the amount of heat required for heating in the cottage heating system, it is necessary to use two wells. The solution of the geometric inverse heat exchange problem to determine the zone of thermal influence of the ground heat exchanger allowed to conclude that the wells must be located at a distance of at least 20 m from each other so that changes in the thermal state of the soil during the heating season do not lead to thermal interference of the wells.

REFERENCES

1 Chen K, Zheng J, Li J, Shao J, Zhang Q. Numerical study on the heat performance of enhanced coaxial borehole heat exchanger and double U borehole heat exchanger. Applied Thermal Engineering [Internet]. 2022 Feb; 203:117916. Available from: http://dx.doi.org/10.1016/j.applthermaleng.2021.117916

2 Lekić Brettschneider A, Perković L. Numerical analysis of borehole heat exchanger performance in shallow gravel aquifers and clay-dominated soil. Rudarsko-geološko-naftni

zbornik [Internet]. 2024; 39(2):75–84. Available from: http://dx.doi.org/10.17794/rgn.2024.2.6
3 Heat transfer in borehole heat exchangers. Computational Modeling of Shallow Geothermal Systems [Internet]. 2011 Sep 30; 49–56. Available from: http://dx.doi.org/10.1201/b11462-10
4 Wang C, Fu Q, Fang H, Lu J. Estimation of Ground Thermal Properties of Shallow Coaxial Borehole Heat Exchanger Using an Improved Parameter Estimation Method. Sustainability [Internet]. 2022 Jun 16; 14(12):7356. Available from: http://dx.doi.org/10.3390/su14127356
5 Luo Y, Guo H, Meggers F, Zhang L. Deep coaxial borehole heat exchanger: Analytical modeling and thermal analysis. Energy [Internet]. 2019 Oct; 185:1298–313. Available from: http://dx.doi.org/10.1016/j.energy.2019.05.228
6 Gustafsson AM, Westerlund L. Heat extraction thermal response test in groundwater-filled borehole heat exchanger – Investigation of the borehole thermal resistance. Renewable Energy [Internet]. 2011 Sep; 36(9):2388–94. Available from: http://dx.doi.org/10.1016/j.renene.2010.12.023
7 Jahangir MH, Sarrafha H, Kasaeian A. Numerical modeling of energy transfer in underground borehole heat exchanger within unsaturated soil. Applied Thermal Engineering [Internet]. 2018 Mar; 132:697–707. Available from: http://dx.doi.org/10.1016/j.applthermaleng.2018.01.020
8 Sun L, Fu B, Wei M, Zhang S. Analysis of Enhanced Heat Transfer Characteristics of Coaxial Borehole Heat Exchanger. Processes [Internet]. 2022 Oct 12; 10(10):2057. Available from: http://dx.doi.org/10.3390/pr10102057
9 Kerme ED. Transient Heat Transfer Modeling, Simulation and Performance Analysis of Single and Double U-Tube Borehole Heat Exchanger. 2024 Feb 20; Available from: http://dx.doi.org/10.32920/25234750
10 Beier RA. Transient heat transfer in a U-tube borehole heat exchanger. Applied Thermal Engineering [Internet]. 2014 Jan;62(1):256–66. Available from: http://dx.doi.org/10.1016/j.applthermaleng.2013.09.014
11 Geotechnical investigation and testing. Geothermal testing. Determination of thermal conductivity of soil and rock using a borehole heat exchanger. Available from: http://dx.doi.org/10.3403/30284748
12 Lamarche L. Ground Heat Exchanger Modeling, Outside the Borehole. Fundamentals of Geothermal Heat Pump Systems [Internet]. 2023; 57–72. Available from: http://dx.doi.org/10.1007/978-3-031-32176-4_4
13 Soriano G, Siguenza D. Thermal Performance of a Borehole Heat Exchanger Located in Guayaquil-Ecuador Using Novel Heat Transfer Fluids. Volume 6A: Energy [Internet]. 2015 Nov 13; Available from: http://dx.doi.org/10.1115/imece2015-51468
14 Gao Y, Zhang W, Yao H, Zhang Z, Cui P, Yu M. Investigation of the Heat Transfer of a Single U-Tube Borehole Heat Exchanger for Medium-Shallow Geothermal Energy. 2024; Available from: http://dx.doi.org/10.2139/ssrn.4880242

IRSTI 52.47

IMPROVEMENTS IN DETAILED CHARACTERISATION OF LOW PERMEABILITY PETROLEUM RESERVOIRS

Ivakhnenko A.P.[1], Nadirov K.S.[2*], Bimbetova G.Zh.[2]
[1]*IPEC, Edinburgh, United Kingdom*
[2]*M. Auezov South Kazakhstan State University, Shymkent, Kazakhstan*
[*]***Corresponding Author's Email:*** *nadirovkazim@mail.ru*

ABSTRACT

Applications of magnetic petrophysics in petroleum engineering demonstrate new potential advantages for the oil and gas reservoir characterisation. In particular, petrophysical magnetic hysteresis method can provide rapid, improved, non-destructive characterisation of multiple mineral and fluid components for oil and gas field characterisation. The advantage of the hysteresis methods is identification of multiple mineral components in the petroleum reservoir samples, by acquiring data at a range of low and high applied magnetic fields. The results demonstrate importance of using this new technology for detailed reservoir analysis. Formation waters and injected sea water, which was pumped through the injected wells into the reservoirs, were also studied. All the fluids were free of solids, such as sand, clay and carbonate sediments or other fluid contamination. For magnetic susceptibility measurements were used very sensitive measuring equipment comprising a magnetic susceptibility balance.

Keywords*:* oil and gas reservoir characterisation, petroleum reservoir minerals, magnetic susceptibility, crude oil.

INTRODUCTION

Newly developed petrophysical magnetic hysteresis method can provide rapid, improved, non-destructive characterisation of multiple mineral and fluid components for reservoir characterisation. The advantage of the hysteresis method is identification of multiple mineral components in the petroleum reservoir samples, by acquiring data at a range of low and high applied magnetic fields. Plots of applied magnetic field versus magnetisation, where the slope represents the magnetic susceptibility, provide a universal template upon which any reservoir rock or fluid can be typed and characterised. Pure diamagnetic components, rock matrix minerals such as quartz and calcite, or reservoir fluids, such as crude oils and formation waters, are characterised by straight lines with negative slope. In contrast, the pure paramagnetic components, permeability controlling clays such as illite and chlorite display straight lines with positive slope. Mixtures of diamagnetic and paramagnetic minerals can be theoretically modelled and compared with experimental results on the plots. The presence of characteristic hysteresis loops at relatively low fields enable very small concentrations of ferri- or ferromagnetic minerals, such as magnetite or hematite to be also rapidly identified. The presence of multiple components, such as diamagnetic, paramagnetic and ferromagnetic types in the same reservoir core can be recognised by distinctive changes in the slope of the hysteresis curves as a function of applied field. Furthermore, magnetic remanence measurements can independently identify the magnetic remanence carrying ferro- or ferrimagnetic particles without any influence from the diamagnetic or paramagnetic components, which do not acquire a remnant magnetisation. As a result the hysteresis and remanence measurements have allowed very sensitive characterisation of different reservoir rock and fluid types to be made. The techniques allow distinguishing subtle variations in the clastic reservoirs, different carbonate types and different reservoir fluids.

The advantage of the hysteresis measurements on reservoir samples is that the magnetic susceptibility can be determined at a range of low and high applied fields. This allows distinguishing different mineral components in a sample as detailed further. Hysteresis curves are plotted on graphs of applied magnetic field versus magnetisation, and in the present work the applied field ranged up to almost 1000 mT. On these plots the magnetic susceptibility is given by the slope of the graph. Changes in the slope for a given sample can indicate the presence of multiple components in the sample. Diamagnetic minerals (quartz, calcite, kaolinite) or fluids (most crude oils and formation waters) are recognised by exhibiting straight lines with negative slope. In contrast, paramagnetic minerals (illite, chlorite) will exhibit a straight line with positive slope. A mixture of a diamagnetic matrix mineral, such as quartz and a paramagnetic clay mineral, such as illite, will have a slope that is dependent upon the content of the two minerals.

MATERIALS AND METHODS

Magnetic methods are well-known in the area of petroleum engineering and geoscience. They have clear advantages for usage in the petroleum industry applications, including high resolution and rapidity of measurements 28T[1,3]28T. However, there is very limited data about the magnetic susceptibility of the reservoir fluids, such as crude oils and formation waters. Recent studies by 28T[2] 28T showed that among crude oil components the most diamagnetic compounds are the alkanes, and the least diamagnetic hydrocarbon compounds are the aromatic hydrocarbons such as benzol with its homologues, naphtheno-aromatic and polycyclic aromatic hydrocarbons. Cyclopentane and cyclohexane hydrocarbons populate intermediate positions between the most and the least diamagnetic hydrocarbon compounds. Alkanes with cyclopentanes and cyclohexanes ranged in value from about -1.00 to -1.13 (10P^{-8}P mP^{3}P kgP^{-1}P). Aromatic hydrocarbons have a magnetic susceptibility range of -0.85 to -0.97 (10P^{-8}P mP^{3}P kgP^{-1}P). In contrast, the oxygen and nitrogen compounds were significantly less diamagnetic. In general, the sulphur crude oil components exhibit a susceptibility range similar to that of the benzol homologues.

Hydrocarbon reservoirs contain a variety of naturally occurring fluids, including heavy and light oils, gas condensates, formation waters. The results in this study consider the main types of natural reservoir fluids in liquid form: crude oils and formation waters. A suite of representative samples of fresh crude oil were collected mainly from different oil fields from world oil provinces, including Middle East, North America, the Far East and Russia. The samples of crude were chosen with a range of distinctive physical and chemical differences. The fluids were kept in their sealed containers until a few days before the measurements when they were poured into glass sealed tubes.

Formation waters and injected sea water, which was pumped through the injected wells into the reservoirs, were also studied. All the fluids were free of solids, such as sand, clay and carbonate sediments or other fluid contamination. For magnetic susceptibility measurements were used very sensitive measuring equipment comprising a magnetic susceptibility balance.

RESULTS AND DISCUSSION

Analysis of the magnetic susceptibilities of the natural reservoir fluids demonstrates that the magnetic susceptibilities of all the studied fluids are diamagnetic. Results show that the mass magnetic susceptibility of crude oils is changing in generals from a value of -0.9634 to -1.0401 (10P^{-8}P mP^{3}P kgP^{-1}P). The magnetic susceptibility of this range of crude oils differs by no more than 7.4% in their magnetic susceptibility values. The formation waters show a distinctly different range from -0.8729 to -0.8862 (10P^{-8}P mP^{3}P kgP^{-1}P). Formation waters vary by 1.5%.

Formation waters are distinctly different from the crude oils (around 12%) in terms of their average magnetic susceptibilities. This demonstrates that there is a real difference between the magnetic susceptibility of the crude oils and the formation waters that would allow us to use this for the reservoir fluid detection, in particular in new logging tools.

Mass magnetic susceptibility has also good correlation with the density of the natural reservoir fluids. There is a trend of higher density corresponding to less negative mass magnetic susceptibilities, with a clear difference between the oils and the formation waters.

In relation to stock tank oil gravity there is also a distinct trend of decreasing mass magnetic susceptibility with increasing gravity. This trend is consistent with the expected trend on the basis of the susceptibility versus density results. Stock tank oil is oil as it exists at atmospheric conditions in a stock tank (it tends to lack much of the dissolved gas present at reservoir temperatures and pressures). The gravity is expressed as API degrees by the following equation below,

$$P^{o}PAPI = [141.5 / SR_{o}R] - 131.5$$

where SR$_{o}$R is the stock tank oil specific gravity, or relative density, to water at 298 K, and API is an acronym for American Petroleum Institute. For a value of 10P^{o}P API, SR$_{o}$R is 1.0, the specific gravity of water.

The values of the API gravity form the common basis of the oil classification system (Table 1). Results demonstrate that the magnetic susceptibility and API gravity are related to each other. Therefore, it appears possible use magnetic susceptibility for oil type classification. In general Table 1 shows that tar with API gravity less than 10P^{o}P is characterized by mass susceptibility values higher than -0.9592 (10P^{-8}P mP^{3}P kgP^{-1}P). Heavy oils correspond to susceptibility in the range -0.9592 to -0.9952 (10P^{-8}P mP^{3}P kgP^{-1}P). Black low shrinkage and volatile high shrinkage oils are characterized by mass susceptibility ranges of -1.0072 to -1.0312 and -1.0312 to -1.0552 (10P^{-8}P mP^{3}P kgP^{-1}P) respectively.

Table 1. Magnetic susceptibility ranges of crude oils.

Reservoir fluid	API gravity	Mass magnetic susceptibility (10P^{-8}P mP^{3}P kgP^{-1}P)
Tar	<10P^{o}	>-0.9592
Heavy oil	10P^{o}P-25P^{o}	-0.9592 - -0.9952
Black low shrinkage oil	30P^{o}P-40P^{o}	-1.0072 - -1.0312
Volatile high shrinkage oil	40P^{o}P-50P^{o}	-1.0312 - -1.0552

It is important to consider the magnetic susceptibilities of crude oils and formation waters in relation to some typical petroleum reservoir minerals, such as the diamagnetic matrix minerals. The comparisons are shown in Fig. 1. The reservoir mineral data comes from previously published experimental results. The average values of the mass magnetic susceptibilities of the reservoir fluids are comparable but different in relation to the diamagnetic susceptibilities of the main matrix minerals, such as quartz, calcite shown in Fig. 1. However, they are distinctly different from the higher positive values of the paramagnetic reservoir minerals such as clays.

Magnetic susceptibility has potential applications to use in passive sensors in reservoirs for distinguishing between formation waters and crude oils. This is important for determination the onset of water breakthrough. Such sensors would provide an environmentally friendly alternative to radioactive tracers. Although viscosity meters might also distinguish between formation waters and crude oils, the magnetic sensors have a further advantage in that they could also rapidly detect small concentrations of ferrimagnetic minerals or migrating fines (such as paramagnetic clays).

Since magnetic susceptibilities of the natural reservoir fluids are more negative than the majority of the diamagnetic matrix reservoir minerals such as quartz, feldspar and calcite, and at the same time the values are significantly less diamagnetic than the clay kaolinite, it appears that magnetic properties will allow typing fluids and minerals in rock-fluid interactions. The relative magnetic forces between quartz and formation water and between quartz and crude oil, in the Earth’s field, might be a factor in determining the wettability of the reservoir rock. For reservoir rocks containing significant amounts of paramagnetic clays, such as illite, the relative magnetic roles of formation water and crude oil could be reversed, most likely influencing the changes in wettability that one often observes between clean sandstone and muddy sandstones containing paramagnetic clays.

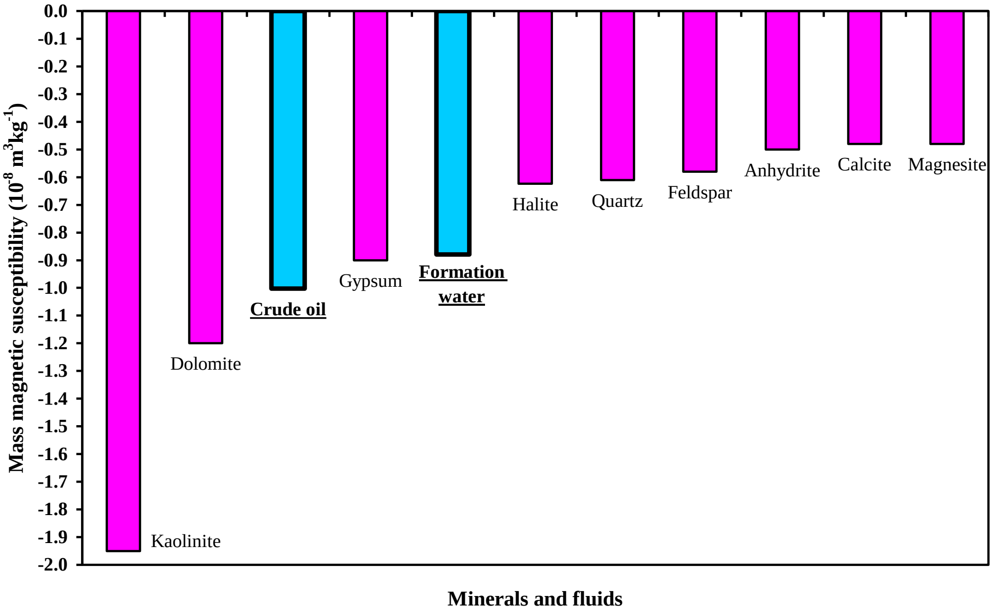

Fig. 1. Magnetic susceptibility of typical reservoir diamagnetic minerals and reservoir fluids.

We studied plots of applied magnetic field versus magnetisation, where the slope represents the magnetic susceptibility, provide a universal template upon which any reservoir rock or fluid can be typed and characterised. Pure diamagnetic components, rock matrix minerals such as quartz and calcite, or reservoir fluids, such as crude oils and formation waters, are characterised by straight lines with negative slope. In contrast, the pure paramagnetic components, permeability controlling clays such as illite and chlorite display straight lines with positive slope. Mixtures of diamagnetic and paramagnetic minerals can be theoretically modelled and compared with experimental results on the plots. The presence of characteristic hysteresis loops at relatively low fields enable very small concentrations of ferri- or ferromagnetic minerals, such as magnetite or hematite to be also rapidly identified. The presence of multiple components, such as diamagnetic, paramagnetic and ferromagnetic types in the same reservoir core can be recognised by distinctive changes in the slope of the hysteresis curves as a function of applied field. Furthermore, magnetic remanence measurements can independently identify the magnetic remanence carrying ferro- or ferrimagnetic particles without any influence from the diamagnetic or paramagnetic components, which do not acquire a remnant magnetisation. As a result the hysteresis and remanence measurements have allowed very sensitive characterisation of different reservoir rock and fluid types to be made. The techniques allow distinguishing subtle variations in the clastic reservoirs, different carbonate types and different reservoir fluids.

The advantage of the hysteresis measurements on reservoir samples is that the magnetic susceptibility can be determined at a range of low and high applied fields. This allows distinguishing different mineral components in a sample as detailed further. Hysteresis curves are plotted on graphs of applied magnetic field versus magnetisation, and in the present work the applied field ranged up to almost 1000 mT. On these plots the magnetic susceptibility is given by the slope of the graph. Changes in the slope for a given sample can indicate the presence of multiple components in the sample. Diamagnetic minerals (quartz, calcite, kaolinite) or fluids (most crude oils and formation waters) are recognised by exhibiting straight lines with negative slope. In contrast, paramagnetic minerals (illite, chlorite) will exhibit a straight line with positive slope. A mixture of a diamagnetic matrix mineral, such as quartz and a paramagnetic clay mineral, such as illite, will have a slope that is dependent upon the content of the two minerals. We theoretically modelled response of different quartz plus illite mixtures on a hysteresis plot that is shown in Fig. 2. This shows that, whilst pure quartz has a relatively steep negative slope, small increases in illite content can have a dramatic effect on the slope of the hysteresis curve. In particular, just 4-5% illite content can cause the slope of the quartz plus illite mixture to become positive. Differences in the slopes of the hysteresis curves for different reservoir samples can potentially allow very sensitive and subtle changes in the magnetic mineralogy to be readily recognised. This is important, for instance, since small changes in illite content can significantly affect fluid permeability. These mineralogical changes may not be necessarily be readily identified by other methods, including XRD, which is generally regarded as semi-quantitative.

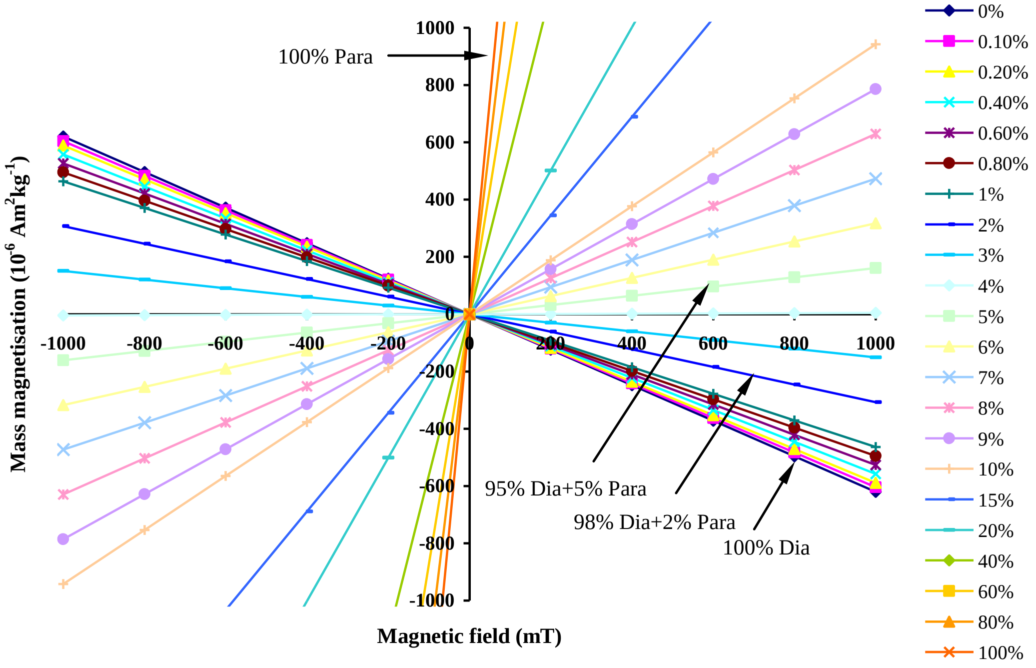

Fig 2. Theoretical models of magnetic hysteresis curves for various mixtures of illite and quartz reservoir sandstones. Selected diamagnetic (Dia) and paramagnetic (Para) mixtures are shown for clarity. 100% Dia refers to pure diamagnetic quartz and 100% Para refers to pure paramagnetic illite.

The majority of ferro- or ferrimagnetic minerals saturate in fields much lower than the maximum field used in the present experiments (1000 mT). The presence of such minerals therefore causes characteristic hysteresis “loops” in the low field region of the graphs. The magnetic measurements allow these minerals to be quickly and non-destructively detected even when they occur in such small quantities that they may not be seen by destructive XRD.

Example of clastic reservoir rock samples is represented by a clean sandstone and a muddy sandstone from the same reservoir. Hysteresis curves for the two studied samples reveal clear differences that can be explained by the relative amounts of the different mineral components they contain. Sample of clean sandstone exhibits an almost straight line with a steep negative slope. This demonstrates that the sample consists primarily of a diamagnetic mineral. This is consistent with the fact that this sample is a clean sand, essentially diamagnetic quartz. The slight "loop" in the curve at low applied field indicated the presence of a very minute amount of a ferrimagnetic mineral. Sample of muddy sandstone also exhibits a negative slope at high fields, indicating a predominant diamagnetic component, again quartz in this case, but the slope is less negative that for the sample of clean sandstone. This suggested an increased contribution from paramagnetic components in the rock of muddy sandstone. It is consistent with this sample having shally components, with a slightly higher content of paramagnetic illite clay. Also the more pronounced hysteresis "loop" at low applied fields demonstrated an increased ferrimagnetic component in sample of muddy sandstone compared to sample of clean sandstone.

The vast majority of reservoir fluids are diamagnetic. As shown above and by Ivakhnenko et al (2004) there are identified clear differences between crude oils and formation waters on the basis of single magnetic reading measurements from a magnetic susceptibility balance, as well as more detailed measurements using a superconducting quantum interference device magnetometer. Hysteresis measurements have confirmed these differences. The study demonstrates that a crude oil sample from the Dunbar Field in the North Sea exhibits a steeper negative slope (more diamagnetic susceptibility) than a formation water sample from the same field. The results were consistent with the previous data obtained independently from the MSB and SQUID magnetometer (Ivakhnenko and Potter, 2004). For comparison, were studied data for kaolinite, quartz and illite using quoted values of susceptibility and reservoir rock samples. Therefore, mineral distinctions displayed in these type of plots are very important and useful as a general template for characterising any petroleum reservoir rock or fluid samples, especially in low permeability petroleum reservoirs.

CONCLUSION

It was confirmed that there were distinct differences between the magnetic susceptibilities of crude oils and formation waters. All fluids were diamagnetic, but the values for the crude oils were more negative diamagnetically. The values of magnetic susceptibility for the crude oils and formation waters correlated with their densities and API gravity. It was also demonstrated that the magnetic susceptibilities of the reservoir fluids are much closer in value to the main diamagnetic matrix minerals, such as quartz and calcite, than the paramagnetic permeability controlling clay minerals.

The magnetic susceptibility of reservoir fluids appears to be important parameter for rapidly characterising types of reservoir fluids, such as formation water and crude oil. It allows quantitatively and rapidly distinguishing different types of crude oils. Further work may show that this approach is better than the other methods. It is important for detecting major physical properties and the presence of fines and contaminants together with detecting changes in fluids in-situ in the presence of the background reservoir rock matrix signal.

Hysteresis plots of applied magnetic field versus magnetisation from rapid, non-destructive magnetic measurements can be used as a universal template for characterising different reservoir samples. They can help identify multiple mineral components in any reservoir rock sample, and therefore provide another means of reservoir rock typing. Different reservoir fluids can also be distinguished. Changes in the slope and the magnetic susceptibility of the hysteresis curves reflect the different components. At low fields characteristic hysteresis "loops" indicate the presence of ferro- or ferrimagnetic minerals. Straight line sections with negative slope are due to diamagnetic components (such as the matrix minerals quartz and calcite, as well as most reservoir fluids), whilst straight line sections with positive slope are due to paramagnetic components, such as the clay illite. Such straight line sections are generally apparent at high applied fields, where there is no influence from the ferrimagnetic components that generally saturate in lower fields. The relative amounts of paramagnetic and diamagnetic minerals in a reservoir rock, such as paramagnetic clays in a quartz matrix, can be quantified from the slope of the straight line at high fields, and applied for low permeability and other types of oil and gas fields.

REFERENCES

1 Ivakhnenko, O.P. Mineralogical aspects of magnetic-mineralogical model. Journal of Geology, 1999, no. 16, Pages: 24-32.

2 Ivakhnenko, O. P. and Potter, D. K., Magnetic susceptibility of petroleum reservoir fluids. Physics and Chemistry of the Earth, 2004, no. 29, Pages: 899-907.

3 Ivakhnenko, O. P. and Potter, D. K., The use of magnetic hysteresis and remanence measurements for rapidly and non-destructively characterizing reservoir rocks and fluids. Petrophysics, 2008, no. 49, Pages: 47-56.

4 Wang L. Ultra-Low Permeability Reservoirs Ways of Well Pattern Optimization Research. Engineering and Technology Journal [Internet]. 2016 Dec 23; Available from: http://dx.doi.org/10.18535/etj/v1i4.02

5 Gimazov AA, Bazyrov IS. The Development Method of Low-Permeability and Ultra-Low-Permeability Reservoirs by Waterflooding. SPE Russian Petroleum Technology Conference [Internet]. 2021 Oct 12; Available from: http://dx.doi.org/10.2118/206416-ms

6 Zhang L. Investigation on Fiber Assisted Multistage Fracturing of Horizontal Well in Tight Low Permeability Sandstone Reservoirs. Volume 10: Petroleum Technology [Internet]. 2022 Jun 5; Available from: http://dx.doi.org/10.1115/omae2022-79132

7 Law A, Megson J, Pye M. Low permeability reservoirs: introduction. Petroleum Geoscience [Internet]. 2001 Mar;7(1):2–2. Available from: http://dx.doi.org/10.1144/petgeo.7.1.2

8 Law A, Megson J, Pye M. Low permeability reservoirs: introduction. Petroleum Geoscience [Internet]. 2001 Mar;7(1):2–2. Available from: http://dx.doi.org/10.1144/petgeo.7.1.2

9 Minkyu Lee JH. Experimental Investigation of Polymer Adsorption-Induced Permeability Reduction in Low Permeability Reservoirs. Journal of Petroleum &

Environmental Biotechnology [Internet]. 2014;05(04). Available from: http://dx.doi.org/10.4172/2157-7463.1000183

10 Liu S, Xiao W, Yang LH, Jiang JH. Numerical Simulation of the Mutative Permeability Effect of Percolation on Low-Permeability Reservoirs. Petroleum Science and Technology [Internet]. 2011 Aug 18;29(20):2151–9. Available from: http://dx.doi.org/10.1080/10916466.2011.585355

11 Wei Z, Sheng JJ. Study of thermally-induced enhancement in nanopores, microcracks, porosity and permeability of rocks from different ultra-low permeability reservoirs. Journal of Petroleum Science and Engineering [Internet]. 2022 Feb;209:109896. Available from: http://dx.doi.org/10.1016/j.petrol.2021.109896

12 ZHANG S, FANG Z. Permeability damage micro-mechanisms and stimulation of low-permeability sandstone reservoirs: A case study from Jiyang Depression, Bohai Bay Basin, China. Petroleum Exploration and Development [Internet]. 2020 Apr;47(2):374–82. Available from: http://dx.doi.org/10.1016/s1876-3804(20)60054-4

IRSTI 61.13

MANUFACTURE OF FURFURYL ALCOHOL BASED ON HETEROCYCLIC OXYGEN-CONTAINING COMPOUNDS

Khaldarov N.Kh.[1*], Rakhimov M.N.[2], Kilibaeva A.E.[1], Egemberdieva S.Zh.[1]
[1]*M. Auezov South Kazakhstan State University, Shymkent, Kazakhstan*
[2]*Ufa State Oil Technical University, Ufa, Russia*
[*]***Corresponding Author's Email:*** *haldarov.nartai@mail.ruU39T*

ABSTRACT

Furfural is the initial object for the synthesis of new compounds that are widely used in the chemical, textile, construction, engineering and aviation industries. Currently, in the CIS countries furfuryl alcohol is produced on an oxide copper - chromite catalyst. This catalyst does not meet modern requirements for activity, selectivity and stability. Therefore, the development of high-performance catalysts and technology for the production of furfuryl alcohol with their use on the basis of local raw materials is an urgent task of great economic importance.

The development of technology for the production of furfuryl alcohol using copper catalysts with the addition of ferroalloys makes it possible to develop a scientific basis for the creation of highly efficient catalysts, and to create new jobs in a socio-economic context and to refuse to import the target product.

Keywords: Furfural, furfuryl alcohol, hydrogenation, catalyst, technology, installation, testing.

INTRODUCTION

Earlier [1-5] we have shown that ferroalloys can be used as modifying additives to increase the catalytic activity of alloy copper catalysts in the reaction of furfural hydrogenation in furfuryl alcohol (FS) under hydrogen pressure.

This report is a continuation of previous studies and is devoted to the study of the effects of the addition of ferromanganese - FMn [an alloy containing (wt.%): 30.22 Fe; 69.0 Mn; 4.3 C; 1.28 Si; 0.20 impurities (P, S)] on the activity of alloyed copper (70% Al) catalyst in the hydrogenation reaction of furfural under hydrogen pressure.

The starting alloys were prepared in a high-frequency melting furnace according to the previously developed technology [6]. The content of components in the alloys was varied (wt.%): Copper - 20-29, aluminum - 70, ferromanganese - 1.0-10.0. The catalysts were obtained from I, 5 g of the alloy by leaching it with a 20% aqueous solution of sodium hydroxide in a boiling water bath for 1 hour.

The phase composition and structure of alloys and catalysts were investigated using X-ray and X-ray methods of analysis; H2 sorption capacity was determined by thermal desorption.

The experiments were carried out in a 250 cm3 Vishnevsky autoclave with vigorous stirring [6]. 200 cm3 of a 10% aqueous solution of furfural and 0.45 g of a leached catalyst were used for hydrogenation. The temperature of the experiment was varied from 40 to 1200C, the hydrogen pressure was in the range of 4-12 MPa. The products of hydrogenation were analyzed in a chromatograph with a flame ionization detector. The activity of the suspended catalysts was judged by the rate of hydrogenation (W), expressed in g of PS per 1 g of catalyst for 1 hour (W,g/g•h).

The optimal composition of catalysts was tested in a steady state for continuous hydrogenation of furfural (without solvent) in an integrated laboratory plant of the column type [6]. The industrial catalyst GIPH-105 was activated by restoring it directly in the reactor in a stream of hydrogen at 1200 ° C for 3 hours. The activity of stationary catalysts was judged by the magnitude of their contact loads, expressed in l of hydrogenated furfural per liter of catalyst for 1 hour (W, l / l • h or $hP^{-1}P$), corresponding to 98-100% FS output. The stationary catalyst was regenerated with a decrease in the PS yield to 95–96%.

MATERIALS AND METHODS

Raw Materials:

Furfural (purity ≥ 99%) was used as the primary feedstock for the synthesis of furfuryl alcohol. Hydrogen gas (H_2, purity ≥ 99.9%) was employed as the reducing agent. Heterocyclic oxygen-containing compounds, such as tetrahydrofuran (THF) and γ-valerolactone (GVL), were used as solvents and co-catalysts.

Catalysts: Copper-chromium oxide (Cu-Cr-O), nickel-based catalysts, and supported palladium catalysts (Pd/Al_2O_3) were utilized for the hydrogenation process.

Chemicals and Reagents: All chemicals and solvents were of analytical grade and used without further purification unless otherwise stated.

Catalyst Preparation:

The Cu-Cr-O catalyst was prepared by co-precipitation of copper and chromium nitrates, followed by calcination at 400°C for 4 hours. The Pd/Al_2O_3 catalyst was synthesized by impregnating alumina with a palladium chloride solution, followed by reduction under hydrogen flow at 300°C.

Hydrogenation of Furfural: The hydrogenation reactions were carried out in a high-pressure batch reactor equipped with a magnetic stirrer and temperature control system. Furfural was dissolved in a selected solvent (THF or GVL) and introduced into the reactor along with the catalyst. The reactor was purged with nitrogen to remove air, followed by pressurization with hydrogen to the desired pressure (10–50 bar). The reaction was conducted at temperatures ranging from 100°C to 200°C for 2–6 hours under continuous stirring.

Product Analysis: The reaction products were analyzed using gas chromatography (GC) equipped with a flame ionization detector (FID) and a capillary column (e.g., HP-5).

The identification of furfuryl alcohol and by-products was confirmed by gas chromatography-mass spectrometry (GC-MS). The conversion of furfural and the selectivity toward furfuryl alcohol were calculated based on the GC data. Optimization of Reaction Conditions: The effects of temperature, hydrogen pressure, catalyst loading, and solvent type on the conversion and selectivity were systematically investigated. Response surface methodology (RSM) was employed to optimize the reaction parameters for maximum yield of furfuryl alcohol.

Catalyst Characterization: The catalysts were characterized using X-ray diffraction (XRD), scanning electron microscopy (SEM), and Brunauer-Emmett-Teller (BET) surface area analysis to study their structural and textural properties. Temperature-programmed reduction (TPR) was performed to evaluate the reducibility of the catalysts. Recycling of Catalysts: The reusability of the catalysts was tested by recovering and regenerating them after each reaction cycle. The spent catalysts were washed with ethanol, dried, and calcined before reuse.

RESULTS AND DISCUSSION

The results of the study of the physicochemical and adsorption properties of the initial alloys and catalysts show that the addition of ferromanganese in the alloys form difficult to leach inclusions, crush the crystals of sklett copper, increase the specific surface, pore volume and the value of their effective radii, hydrogen sorption. All this has a positive effect on the activity of the studied catalysts.

Data on the hydrogenation of furfural at 900 ° C and 6 MPa on skeletal copper (70% Al) catalysts with the addition of ferromanganese are presented in Table 1.

Table 1. Hydrogenation of furfural on alloyed copper (70% Al) catalysts with the addition of ferromanganese. Conditions: 200 cm3 of a 10% aqueous solution of furfural; 900C and 6 MPa, 0.45 g of catalyst

Additive FMn, wt.%	PC output (%) in time (min.)				W, g / g•h
	10	20	40	60	
1	2	3	4	5	6
Cu (70% Al)	-	0.9	4.3	8.7	4.8
1.0% FMn	15.0	20.4	36.0	49.0	22.2
3.0	18.0	27.3	45.4	57.3	23.4
5.0	22.0	32.0	47.0	61.3	27.8
10.0	18.5	22.0	37.6	51.3	23.3

From the data Table 1 it can be seen that the hydrogenation of furfural on the studied Cu-FMn (70% Al) catalysts is carried out selectively to PC, the formation rate of which is 4.6 - 5.8 times higher, on skeletal Cu (70% Al) without an additive. The most active catalyst is an alloy of 5.0 wt.% FMn, the output of the PC, which for 60 min. hydrogenation reaches 61.3%.

The promoting effect of FMn additives is due to a change in the phase composition, the porous structure of the catalysts, as well as an increase in their sorption capacity with respect to hydrogen. In addition, according to [7], the addition of iron and manganese in the form of FMn has an acceptor effect on copper, which enhances the n-coordination of the furfural molecule with the surface and weakens the strength of the Cu + N bond [4].

Next, we studied the effect of hydrogen pressure and temperature of experiment on the rate of hydrogenation of furfural in the presence of a Cu-5% FMn (70% Al) catalyst. The results are shown in Table 2.

From the data table. 2 it follows that a simultaneous increase in the pressure of hydrogen from 4 to 12 MPa, the temperature of the experiment within 40-1200C causes an increase in the rate of formation of FS by 2.0 - 8.2 times.

Table 2. Effect of test temperature and hydrogen pressure on the activity of skeletal Cu-5% FMn (70% Al) catalyst. Conditions: 200 cm3 of a 10% aqueous solution of furfural; 0.45 g of catalyst

t, °C	PR$_{H2}$R, MPa	PC output (%) in time (min.)				W, g / (g. h)	KR$_{cr}$R, hP^{-1}	Order by HR$_2$R
		10	20	40	60			
1	2	3	4	5	6	7	8	9
40	4	2.0	4.0	6.7	11.2	5.1	1.6378	0.8
	12	7.0	12.4	22.0	30.5	13.8		0.8
60	4	8.0	13.0	25.0	33.0	15.7	6.0022	0.7
	12	27.0	42.5	63.4	76.0	34.5		0.7
90	4	15.7	21.0	37.0	50.0	22.7	9.1380	0.6
	12	49.6	63.4	85.4	94.0	42.6		0.6
100	4	18.5	29.0	47.0	59.0	26.8	13.7226	0.5
	12	50.0	66.0	87.0	96.0	43.5		0.4
120	4	23.4	31.0	56.4	67.0	30.4	18.4139	0.4
	12	52.4	72.0	94.0	100.0	45.4		03

A continuous hydrogenation of furfural without solvent was carried out on a stationary Cu-70% Al-5% FMn catalyst under conditions of varying technological parameters. The results are shown in table 3. From the data table. 3 shows that the only product of the process of continuous hydrogenation of furfural on the stationary catalyst under study is a PS, the yield of which reaches 98-100%.

Table 3. Continuous hydrogenation of furfural (without solvent) on stationary Cu-70% Al-5% FMn catalyst

Leach rate Al, %	V cat. cmP^3	tP^{0}P C	PR$_{H2}$ R, MPa	WR$_{H2}$ R, hP^{-1}	WR$_{ff}$ R, hP^{-1}	Reaction products output, %		Relative duration process, h.
						FF	FS	
Cu – Al = 30 – 70								
30.0	80.0	100-140	4	180	0.142-0.142	0.0-7.0	90.3-100	132
Cu - 70% Al - 5% FMn								
30.0	80.2	80-140	4	180	0.385-0.52	0.0-2.0	98-100	492
35.0	77.6	120	2-8	180	0.41-0.56	0.0-1.5	98.5-100	484
40.0	75.0	120	4	10-180	0.460 0.58	0.0-2.0	98-100	475
Industrial HYPH-105								
Restore.at 120P^{0}PS in tech.3 hours	90.0	90-120	4	180	0.200	0.0-15.0	85-100	260

The values of contact loads for stationary Cu-70% Al-5% FMn catalyst reaches 0.385-0.580 h - 1, which is 1.9-2.7 times higher than that of industrial GYPH -105 contact. With depth, the leaching of aluminum from 30 to 40%, the temperature of the experience in the range of 80-140P^{0}PS, the hydrogen pressure is from 2 to 8 MPa, the speed of bubbling of hydrogen in the range of 10-180h-1 contact load of the investigated alloy of copper catalyst increases to 1.18-1.32 times. It should be noted that as the depth of aluminum leaching from the catalyst increases, the duration of the process decreases within 492-475h. The stability of the investigated alloy catalyst with the addition of FMn is 1.8-1.85 times higher than that of the industrial HYPH - 105 contact.

CONCLUSION

1. Hydrogenation of furfural on copper alloy (70% Al) catalysts with the addition of ferromanganese was transferred. It has been established that hydrogenation of furfural occurs selectively to PS, the formation rate of which is 4.6–5.8 times higher than that of skeletal Cu (70% Al) without an additive.
2. Simultaneous increase in the process temperature and pressure has a positive effect on the rate of formation of PC. The order of H2 is fractional.
3. A stationary alloyed copper (70% Al) catalyst with the addition of FMn was developed for continuous hydrogenation of furfural in PC, the activity and stability of which is 1.8-1.85 times higher than that of industrial GIPH - 105 contacts.

4. The scientific results obtained will find application in the preparation of catalysts for the hydrogenation of carbonyl-containing compounds of the heterocyclic series.

5.Target consumers of the results obtained in Kazakhstan are manufacturers of petrochemical and agricultural products.

REFERENCES

1 T.B. Beysekov, V.E. Oleynikov, A.A.Meldeshov. Mnogokomponentny`e medny`e katalizatory’ dlya gidrirovaniya furfurola [Multicomponent copper catalysts for hydrogenation of furfural]. Moscow: Nauka, 1990. 132p.

2 T.Beysekov. Katalizatory` dlya gidrirovaniya i dekarbonilirovaniya furfurola [Catalysts for hydrogenation and decarbonylation of furfural]. Shymkent: KazXTI, 1994. 204 p.

3 M.S.Erzhanova, T. Beysekov. Splavny`e katalizatory` dlya gidrirovaniya furfurola [Alloy catalysts for hydrogenation of furfural]. Alma-Ata: Gylym, 1992, 195 p.

4 Beysekov T. Problemy` sovremennogo kataliza na metallax [Problems of modern catalysis on metals]. Almaty: Gylym, 1994. 250 p.

5 Beysekov T.B., Oleynikov V.E., Meldeshov A.A. Gidrirovanie furfurola na mnogokomponentny`x splavny`x medny`x katalizatorax [Hydrogenation of furfural on multicomponent copper alloy catalysts]. Chimkent, BV, 125 p.

6 Mombekov S.A. (1991) Gidrirovanie furanovy`x al'degidov i ketonov na splavny`x medny`x katalizatorov [Hydrogenation of furan aldehydes and ketones on alloyed copper catalysts] (Diss. Chem. Science). Chemical and Technological Institute named after Mendeleev.

7 Dorfman Y.A. Katalizatory` i mexanizmy` gidrirovaniya i okisleniya [Catalysts and mechanisms of hydrogenation and oxidation. Alma-Ata: Science of the Kazakh SSR, 1984, 360p.

8 Synthesis of Oxygen-Containing Heterocyclic Compounds by Iron-Catalyzed Alkylative Cyclization of Unsaturated Carboxylic Acids and Alcohols. Available from: http://dx.doi.org/10.1021/acs.orglett.0c02671.s001

9 Mochalov SS, Gazzaeva RA. Arylcyclopropanes in the Synthesis of Nitrogen- and Oxygen-containing Heterocycles. (Review). Chemistry of Heterocyclic Compounds [Internet]. 2003 Aug;39(8):975–88. Available from: http://dx.doi.org/10.1023/b:cohc.0000003512.21274.e1

10 Venkatachalam H, Venkatesh Anil Kumar N. The Oxygen-Containing Fused Heterocyclic Compounds. Heterocycles - Synthesis and Biological Activities [Internet]. 2020 Jun 10; Available from: http://dx.doi.org/10.5772/intechopen.88026

11 Chapter 4 Amines, Alcohols, Thiols, Ethers, Sulfides, and Heterocyclic Compounds Containing Nitrogen, Oxygen, and Sulfur. Organic Chemistry [Internet]. 2024 4;40–61. Available from: http://dx.doi.org/10.1515/9783111382753-004

12 Liao M, Dong S, Deng G, Wang J. Synthesis of Oxygen-Containing Heterocyclic Compounds Based on the Intramolecular O—H Insertion and Wolff Rearrangement of α-Diazocarbonyl Compounds. ChemInform [Internet]. 2006 Sep 26;37(42). Available from: http://dx.doi.org/10.1002/chin.200642096

IRSTI 61.13.17

THERMAL DECOMPOSITION OF AMMONIA SALTPETER: THE PROCESS KINETICS AND BALANCE, MASS CALCULATIONS

Kydyralieva A.D., Nazarbek U.B.*, Bolysbek A.A.
[1]*M. Auezov South Kazakhstan State University, Shymkent, Kazakhstan*
**Corresponding Author's Email:* unazarbek@mail.ru

ABSTRACT

The research purpose - of the study laws of kinetics and equilibrium of the thermal decomposition of ammonium nitrate, the implementation of material calculations.

An ammonia saltpeter thermal decomposition process was studied with application of a water 50 % solution of the ammonia saltpeter produced by JSC "Kazazot". The process was investigated at changing of the solution temperature from 19 °C to 110 °C at its monotonous growth from 19 °C to 60 °C within 13 minutes, and from 60P P to 110 °C. The total duration of the study was 60 minutes.

In the conditions of experiments, the temperature regime was maintained using a thermostat.The process of thermal decomposition of ammonium nitrate was judged by changing the pH of the solution over time.

On the experimental data of pH at τ = 4; 10.5; 13; 15; 22; 31; 43; 60 minutes calculated molar mass of NHR$_4$RNOR$_3$R is thermally decomposed, the generated NHR$_3$R and NOR$_3$R, the calculated values of the equilibrium constants, degrees of thermal decomposition, speeds process and their relative changes.

The research results have shown, that ammonia saltpeter at all studied temperatures is underwent to thermal decomposition. The process takes place most intensively within the first 30 minutes, and then it slowly reaches the equilibrium condition within the next 30 minutes. Thus the total degree of ammonia saltpeter thermal decomposition makes approximately 4 %.

For all stages of research implemented mass calculations. The calculated results have been processed, represented in diagram form and as tables.

Keywords: ammonium nitrate, explosion hazard, solution temperature, physical and chemical properties, fertilizing properties, agrochemical, the equilibrium constant, of consumer value.

INTRODUCTION

Ammonia saltpeter is one of the product, which is widely applied in many branches of the national economy. At present ammonia saltpeter is produced by many countries of the world. Its technology represents a scientifically substantiated technological decision, completely satisfying modern consumer needs both according to its quality, and the product output.

At the same time, last years both consumers of ammonia saltpeter, and its manufacturers began seriously to think about solving problems of decrease in its fire and explosion hazard, further improvement of physicochemical and fertilizer properties, increase in agrochemical and consumer value.

In addition, as follows from the analysis of literary data, a number of individual properties of ammonia saltpeter should be additionally studied as these properties have an essential effect on its qualitative coefficients and negatively affect technical-economic indicators of the manufacture in whole.

One of such the properties of ammonia saltpeter is its ability to thermal decomposition in molten state [1-4]. As it is known, a temperature factor exerts a very strong impact on a result of polymorphic transformations in structure of ammonia saltpeter [5]. To date, information about kinetic regularities and equilibrium of the processes taking place at ammonium nitrate decomposition at low temperatures is practically absent except individual data [6,7]. For this reason performance of special investigations for studying of laws of the ammonia nitrate decomposition process in a temperature interval below its melting point is an actual problem.

MATERIALS AND METHODS

The investigation has been implemented in laboratory conditions at chair “Chemical technology of inorganic substances” of M. Auezov South Kazakhstan State University using standard test solutions of the ammonia saltpeter produced by joint-stock company “KazAzot” with concentration of 50 % or 7.65 mol/l. The solutions’ temperature at realization of the experiments was maintained from 19 °C to 110 °C during the time sufficient for transition of the ammonia saltpeter thermal decomposition process to final equilibrium condition at 110 °C with application of a thermostat. Changing of the solution pH in time was an indicator of the ammonium nitrate decomposition process.

RESULTS AND DISCUSSION

As follows from the data of Fig 1, at temperature 19 °C initial the investigated solution has pH=5.3. There fore, this ammonia saltpeter solution contains residual surplus nitric acid with concentration of 50.1·10P^{-7} Pmol/l.

Within the next 4 minutes the solution temperature has been increased to 30 °C. In so doing,

the solution pH has decreased to 4.95. The respective calculated value of hydrogen ions concentration [H P^{+}P] = 112·10P^{-7} Pmol/l. In this case the true gain of hydrogen ions concentration is 112·10P^{-7} P– 50.1·10P^{-7} P= 62·10P^{-7} Pmol/l.

After 10.5 minutes from the research initial time the solution temperature has reached 50 °C, pH of the solution has decreased to 4.35, concentration of hydrogen ions was [HP^{+}P] = 447·10P^{-7} Pmol/l, the hydrogen ion concentration gain was 447·10P^{-7}P – 62·10P^{-7}P = 385·10P^{-7}P mol/l.

Within the next 2.5 minutes or after 13 minutes from the beginning of the experiment the solution temperature has reached 60 °C, pH of the solution has decreased to 4.10, hydrogen ion concentration has made [HP^{+}P] = 794·10P^{-7} Pmol/l, and the gain of hydrogen ion concentration – 794·10P^{-7}P – 385·10P^{-7}P = 409·10P^{-7}P mol/l.

After 15 minutes from the beginning of the experiments the solution temperature has reached 110 °C. Thus pH of the solution was 3.9, [HP^{+}P] = 1260·10P^{-7} Pmol/l, the true gain of hydrogen ion concentration for this case was 1260·10P^{-7}P – 409·10P^{-7} P= 851·10P^{-7} Pmol/l.

As the result of further maintenance of the solution constant temperature of 110 °C within the next 7 minutes or after 22 minutes from the beginning of the experiment pH of the solution has decreased to pH=3.0. In this case [HP^{+}P] was 5011.8·10P^{-7} Pmol/l, the gain of hydrogen ion concentration – 5011.8·10P^{-7}P – 851·10P^{-7} P= 4161.8·10P^{-7} Pmol/l.

Then the solution at constant temperature of 110P P°C was subjected to further thermal processing within the next 9 minutes. In so doing after τ=31 minutes from the beginning of the investigation pH of the solution was 3.05, [HP^{+}P] – 8912·10P^{-7} Pmol/l, the true gain of hydrogen ion concentration was 8912·10P^{-7} P– 4161.8·10P^{-7} P= 4750.2·10P^{-7} Pmol/l.

Subsequently the solution temperature was maintained constant at level of 110 °C within the next 29 minutes or 60 minutes from the beginning of the experiment. The solution pH was measured after 43 and 60 minutes. It was found, that in this case the ammonia saltpeter thermal decomposition process is reaching an equilibrium state that is proved by practically complete coincidence of pH values of the solution at τ =43 min and τ =60 min.

On the experimental data of pH at τ = 4; 10.5; 13; 15; 22; 31; 43; 60 minutes calculated molar mass of NHR$_4$RNOR$_3$R is thermally decomposed, the generated NHR$_3$R and NOR$_3$R, the calculated values of the equilibrium constants, degrees of thermal decomposition, speeds process and their relative changes.

The generalized data and results of the conducted researches, results of calculations of equilibrium and kinetic indicators, and also material calculations are represented in Table 1.

Table 1. Generalised data and results of material calculations

№	Time, min	Indicator	Symbol	Unit	Value	Chem. reaction
1	0	Solution concentration Solution temperature Hydrogen ion exponent Hydrogen ion concentration Excess acid concentration Equilibrium constant HNOR$_3$ Rdecomposition degree	$C^{initial}_{NH_4NO_3}$ t pH [HP^{+}P] [HNOR$_3$R] KR$_0$ αR$_0$	mol/l °C - mol/l mol/l mol/l %	7.65 19 5.3 50.1·10P^{-7} 50.1·10P^{-7} 50.1·10P^{-7} 100	HNOR$_3$R ↔ HP^{+}P+NOR$_3$RP^{-}
2	4	Solution concentration Solution temperature Hydrogen ion exponent Hydrogen ion concentration Excess acid concentration Equilibrium constant HNOR$_3$ Rdecomposition degree The process rate	$C^{initial}_{NH_4NO_3}$ t pH [HP^{+}P] [HNOR$_3$R] KR$_4$ αR$_4$ VR$_4$	mol/l °C - mol/l mol/l mol/l % mol/l·min	7.65 30 4.95 112·10P^{-7} 62·10P^{-7} 62·10P^{-7} 0.09 15.5·10P^{-7}	

Table 1 continuation

3	10.5	Solution concentration	$C_{NH_4NO_3}^{initial}$	mol/l	7.6499938	$HNOR_3R \leftrightarrow HP^+P+NOR_3RP^-$
		Solution temperature	t	°C	50	
		Hydrogen ion exponent	pH	-	4.35	
		Hydrogen ion concentration	$[HP^+P]$	mol/l	$447 \cdot 10P^{-7}$	
		Excess acid concentration	$[HNOR_3R]$	mol/l	$385 \cdot 10P^{-7}$	
		Equilibrium constant	$KR_{10.5}$	mol/l	$385 \cdot 10P^{-7}$	
		$HNOR_3$ Rdecomposition degree	$\alpha R_{10.5}$	%	0.22	
		The process rate	$VR_{10.5}$	mol/l·min	$51.5 \cdot 10P^{-7}$	
		Relative change of NHR_4RNOR_3 Rdecomposition degree	$\alpha R_{10,5}R/\alpha R_4$		2.444	
		Relative change of equilibrium constant	$KR_{10.5}R/KR_4$		6.209	
		Relative change of NHR_4RNOR_3 Rdecomposition rate	$VR_{10.5}R/VR_4$		3.32	
4	13	Solution concentration	$C_{NH_4NO_3}^{initial}$	mol/l	7.6499553	$HNOR_3R \leftrightarrow HP^+P+NOR_3RP^-$
		Solution temperature	t	°C	60	
		Hydrogen ion exponent	pH	-	4.10	
		Hydrogen ion concentration	$[HP^+P]$	mol/l	$794 \cdot 10P^{-7}$	
		Excess acid concentration	$[HNOR_3R]$	mol/l	$409 \cdot 10P^{-7}$	
		Equilibrium constant	KR_{13}	mol/l	$409 \cdot 10P^{-7}$	
		$HNOR_3$ Rdecomposition degree	αR_{13}	%	0.23	
		The process rate	VR_{13}	mol/l·min	$163.6 \cdot 10P^{-7}$	
		Relative change of NHR_4RNOR_3 Rdecomposition degree	$\alpha R_{13}R/\alpha R_{10.5}R$		1.045	
		Relative change of equilibrium constant	$KR_{13}R/KR_{10.5}$		1.062	
		Relative change of NHR_4RNOR_3 Rdecomposition rate	$VR_{13}R/VR_{10.5}$		3.17	

Table 1 continuation

5	15	Solution concentration	$C^{cur}_{NH_4NO_3}$	mol/l	7.6499144	NHR$_4$RNOR$_3$R $\downarrow$ $\rightarrow$ R R HP$^+$P+ NOP$^-$PR$_3$R+ NHR$_3$
		Solution temperature	t	°C	110	
		Hydrogen ion exponent	pH	-	3.9	
		Hydrogen ion concentration	[HP$^+$P]	mol/l	1260·10P^{-7}	
		Accumulation of hydrogen ion concentration	[HP$^+$P]	mol/l	851·10P^{-7}	
		Thermally decomposed	NHR$_4$RNOR$_3$	mol	851·10P^{-7}	
		Formed and flown away	NHR$_3$R $\uparrow$	mol	851·10P^{-7}	
		The equilibrium constant	KR$_{15}$	mol/l	851·10P^{-7}	
		Degree of decomposition of NHR$_4$RNOR$_3$	αR$_{15}$	%	0.33	
		The process rate	VR$_{15}$	mol/l·min	425.5·10P^{-7}	
		Relative change of NHR$_4$RNOR$_3$ Rdecomposition degree	αR$_{15}$R/ αR$_{13}$		1.435	
		Relative change of equilibrium constant	KR$_{15}$R/ KR$_{13}$		2.081	
		Relative change of NHR$_4$RNOR$_3$ Rdecomposition rate	VR$_{15}$R/ VR$_{13}$		2.60	

Table 1 continuation

6	22	Solution concentration Solution temperature Hydrogen ion exponent Hydrogen ion concentration Accumulation of hydrogen ion concentration Thermally decomposed Formed and flown away The equilibrium constant Degree of decomposition of NHR_4RNOR_3 The process rate Relative change of NHR_4RNOR_3 Rdecomposition degree Relative change of equilibrium constant Relative change of NHR_4RNOR_3 Rdecomposition rate	$C^{cur}_{NH_4NO_3}$ t pH $[HP^+P]$ $[HP^+P]$ NHR_4R NOR_3 $NHR_3R\uparrow$ KR_{22} αR_{22} VR_{22} $\alpha R_{22}R/\alpha R_{15}R$ $KR_{22}R/KR_{15}R$ $VR_{22}R/VR_{15}$	mol/l °C - mol/l mol/l mol mol mol/l % mol/l·min	7.6498293 110 3.30 $5011.8 \cdot 10P^{-7}$ $4161.8 \cdot 10P^{-7}$ $4161.8 \cdot 10P^{-7}$ $4161.8 \cdot 10P^{-7}$ $4161.8 \cdot 10P^{-7}$ 0.73 $594.5 \cdot 10P^{-7}$ 2.212 7.890 1.40	$NH_4NO_3 \rightarrow H^+ + NO^-_3 + NH_3$

Table 1 continuation

7	31	Solution concentration	$C^{cur}_{NH_4NO_3}$	mol/l	7.64941312	$NH_4NO_3 \rightarrow H^+ + NO_3^- + NH_3$
		Solution temperature	t	°C	110	
		Hydrogen ion exponent	pH	-	3.05	
		Hydrogen ion concentration	[HP$^+$P]	mol/l	8912·10P^{-7}	
		Accumulation of hydrogen ion concentration	[HP$^+$P]	mol/l	4750.2·10P^{-7}	
		Thermally decomposed	NHR$_4$RNOR$_3$	mol	4750.2·10P^{-7}	
		Formed and flown away	NHR$_3$R↑	mol	4750.2·10P^{-7}	
		The equilibrium constant	KR$_{31}$	mol/l	4750.2·10P^{-7}	
		Degree of decomposition of NHR$_4$RNOR$_3$	αR$_{31}$	%	0.79	
		The process rate	VR$_{31}$	mol/l·min	527.8·10P^{-7}	
		Relative change of NHR$_4$RNOR$_3$ Rdecomposition degree	αR$_{31}$R/ αR$_{22}$		1.082	
		Relative change of equilibrium constant	KR$_{31}$R/ KR$_{22}$		1.141	
		Relative change of NHR$_4$RNOR$_3$ Rdecomposition rate	VR$_{31}$R/ VR$_{22}$		0.88	

Table 1 continuation

8	43	Solution concentration Solution temperature Hydrogen ion exponent Hydrogen ion concentration Accumulation of hydrogen ion concentration Accumulation of hydrogen ion concentration Formed and flown away The equilibrium constant Degree of decomposition of NHR$_4$RNOR$_3$ The process rate Relative change of NHR$_4$RNOR$_3$ Rdecomposition degree Relative change of equilibrium constant Relative change of NHR$_4$RNOR$_3$ Rdecomposition rate	$C^{cur}_{NH_4NO_3}$ t pH [HP$^+$P] [HP$^+$P] NHR$_4$R NOR$_3$ NHR$_3$R ↑ КR$_{43}$ αR$_{43}$ VR$_{43}$ αR$_{43}$R/ αR$_{31}$R КR$_{43}$R/ КR$_{31}$ VR$_{43}$R/ VR$_{31}$	mol/l °C - mol/l mol/l mol mol mol/l % mol/l·min	7.6489381 110 3.02 9549·10P^{-7} 4798·10P^{-7} 4798·10P^{-7} 4798·10P^{-7} 4798·10P^{-7} 0.79 400·10P^{-7} 1.000 1.010 0.76	NHR$_4$RNOR$_3$R → R R HP$^+$P+ NOP-PR$_3$R+ NHR$_3$

Table 1 continuation

9	60	Solution concentration Solution temperature Hydrogen ion exponent Hydrogen ion concentration Accumulation of hydrogen ion concentration Thermally decomposed Formed and flown away The equilibrium constant Degree of decomposition of NHR$_4$RNOR$_3$ The process rate Relative change of NHR$_4$RNOR$_3$ Rdecomposition degree Relative change of equilibrium constant Relative change of NHR$_4$RNOR$_3$ Rdecomposition rate	$C^{cur}_{NH_4NO_3}$ t pH [HP$^+$P] [HP$^+$P] NHR$_4$R NOR$_3$ NHR$_3$R ↑ KR$_{60}$ αR$_{60}$ VR$_{60}$ αR$_{60}$R/ αR$_{43}$ KR$_{60}$R/ KR$_{43}$ VR$_{60}$R/ VR$_{43}$	mol/l °C - mol/l mol/l mol mol mol/l % mol/l·min	7.64902276 110 3.02 9549·10P^{-7} 4751·10P^{-7} 4751·10P^{-7} 4751·10P^{-7} 4751·10P^{-7} 0.79 279·10P^{-7} 1.000 0.990 0.70	NHR$_4$RNOR$_3$R ↓ R R HP$^+$P+ NOP$^-$PR$_3$R+ NHR$_3$

CONCLUSION

Ammonia saltpeter may be thermally decomposed both in the field of low temperatures (lower 60 °C) and at raised temperatures (from 60 to 110 °C). The process was investigated at changing of the solution temperature from 19 °C to 110 °C at its within 60 minutes, total degree of ammonia saltpeter thermal decomposition makes approximately 4 %.

On the basis of the conducted research, during which the hydrogen index of the studied solution is used as the determining value of the experimental parameter, it is possible to obtain sufficiently reliable quantitative information about the kinetic and equilibrium parameters of the thermal decomposition of ammonium nitrate, as well as the degree of its thermal decomposition, to perform material calculations of the studied process.

CITATIONS

1. One of such the properties of ammonia saltpeter is its ability to thermal decomposition in molten state [1-4].
2. As it is known, a temperature factor exerts a very strong impact on a result of polymorphic transformations in structure of ammonia saltpeter [5].
3. To date, information about kinetic regularities and equilibrium of the processes taking place at ammonium nitrate decomposition at low temperatures is practically absent except individual data [6,7].

REFERENCES

1 Robertson P.I. The thermal decomposition of PETN, NG, EDADN and ammonium nitrate. *J.Phys. Chem. Ind*, 1948, issue 67, Pages: 221-224.

2 Rosser W.A., Inami S.H., Wise H. The kinetics of decomposition of liquid ammonium nitrate. *J. Phys. Chem*. 1963, issue 67, no. 9, Pages: 1753-1757.

3 Rubtsov A.I., Kazakov N.G., Morozkin S.Ju. Kinetics of heat generation at technical ammoniac saltpeter thermal decomposition. *Applied Science Journal*, 1984, issue 57, no. 57, no. 9, Pages: 1926-1929.

4 Usmonov K.P., Mamatkulov A.M., Emirsaliyev S.S., Pochitalkina I.A., Kondakov D.F. Polymorphic transformations and properties of the ammonia saltpeter samples modified by inorganic additives. *Successes in chemistry and chemical technology*, issue 25, 2011, no. 8 (124), Pages: 61-64.

5 Bespalov G.N., Filatova L.B., Shidlovsky A.A. About thermal decomposition of ammonium nitrate. *Journal of physical chemistry*. 1968, issue 42, no 10, Pages: 2623-2627.

6 Moshkovich E.B., Podshivalova G.N., Sidorina I.Ju., Strizhevsky I.I. Thermo-decomposition of ammonia saltpeter at temperatures below its melting temperature. *Applied Science Journal*, 1982, issue 55, Pages: 901-905.

7 Besterekov U, Kydyralieva AD, Petropavlovskiy IA, et al. Mass balance calculations of processes of ammonia saltpeter thermal decomposition and nitric acid absorption of ammonia. Bulletin of the Karaganda University “Chemistry” series [Internet]. 2019 Dec 30;96(4):92–7. Available from: http://dx.doi.org/10.31489/2019ch4/92-97

8 REED AV. Fuel Retrieval System Process Flow Diagrams Mass Balance Calculations for K West Basin [Internet]. Office of Scientific and Technical Information (OSTI); 2000 Jan. Available from: http://dx.doi.org/10.2172/801167

9 Gangal AC, Sharma P. Kinetic Analysis and Modeling of Thermal Decomposition of Ammonia Borane. International Journal of Chemical Kinetics [Internet]. 2013 Apr 25;45(7):452–61. Available from: http://dx.doi.org/10.1002/kin.20781

10 Smith FG. Am/Cm Vitrification Process: Pretreatment Material Balance Calculations [Internet]. Office of Scientific and Technical Information (OSTI); 2001 Feb. Available from: http://dx.doi.org/10.2172/775071

11 Pérez-Maqueda LA, Criado JM, Gotor FJ. Controlled rate thermal analysis commanded by mass spectrometry for studying the kinetics of thermal decomposition of very stable solids. International Journal of Chemical Kinetics [Internet]. 2002 Feb 6;34(3):184–92. Available from: http://dx.doi.org/10.1002/kin.10042

12 Decomposition Kinetics. Thermal Decomposition of Solids and Melts [Internet]. 2007;33–49. Available from: http://dx.doi.org/10.1007/978-1-4020-5672-7_3

IRSTI 61.53.91

DEVELOPMENT OF FLOTATION SEPARATION METHOD OF A MIXTURE FROM MILLED POLYMER WASTES

Opimakh E.V.[1], Levdansky A.E.[1], Volnenko A.A.[2], Daulet K. Zhumadullayev D.K.[2], Zhuk A.M.[2]
[1]*Belorussian State Technological University, Minsk, Belarus*
[2]*M. Auezov South Kazakhstan University, Shymkent, Kazakhstan*
[*]***Corresponding Author's Email:*** *nii_mm@mail.ru*

ABSTRACT

Flotation based on different wettability is a good option for sorting plastics with similar or equal densities and those that are difficult to separate by other methods.

Based on the analysis of the main methods of plastic waste separation, a method for flotation separation of a mixture from milled plastics of various types based on the change in their hydrophilic property or hydrophobicity by supplying surfactants and gas bubbles into the working liquid into its working volume was proposed. A flotation apparatus design was proposed for this method.

The analysis of factors influencing the flotation process with consideration of the apparatus' design parameters, methods for feeding surfactants, mixing, selection of foam and concentrate, as well as technological parameters and physical properties of phases, was carried out.

A list of the flotation process' parameters was determined, which must be specified using mathematical relations or experimentally.

Keywords: flotation, wettability, plastics, surfactants, hydrophilic property, hydrophobicity, design parameters, technological parameters.

INTRODUCTION

To date, the main methods for separating plastic wastes are manual sorting and based on the difference in their density (sedimentation) separation in water using "flotation" chambers [1-7]. The flotation method for separating a mixture of milled plastics in a column apparatus with pneumatic aeration based on different wettability is the most promising for expanding the list of recycled polymer types in different countries.

To create the new method for flotation separation of the mixture of milled plastics of various types, it is proposed to change the hydrophilic property or hydrophobicity of a certain component or components of the mixture of plastics by supplying surfactants and gas bubbles into the working liquid into its working volume. In this case, there is separation of the mixture of milled plastics, which densities may be close to or equal to each other, and greater than the density of the working medium. During the flotation process, the emerged milled particles of the hydrophobic plastic are removed together with the foam in the top of the flotation apparatus as a concentrate, and the settled milled particles of the hydrophilic plastic are removed as a precipitate.

MATERIALS AND METHODS

Standard methods of physicochemical investigations are used to obtain the experimental data.

RESULTS AND DISCUSSION

The flotation separation of the mixture of milled plastics is carried out as follows. The surfactants are supplied into the water-filled flotation apparatus (Figure 1), which is the container *1* of predominantly column type. Through the holes *2* of the aerator *3* located at the flotation apparatus bottom, the gas is supplied, preferably air, which is evenly distributed along the apparatus section in the form of small bubbles *4*. Then, the mixture of milled plastics II is supplied to the flotation apparatus.

In the presence of surfactants and gas bubbles, the hydrophobic particles of milled plastics form “bubble – particle” complexes, the density of which is less than that of the working liquid. These complexes emerge on the working liquid’s surface under the buoyancy force influence. And particles of other types of plastics in the presence of surfactants exhibit hydrophilic properties and fall into the lower flotation apparatus part under the gravitational force influence. The hydrophobic plastics are removed together with foam in the upper flotation apparatus part as the concentrate III, and the hydrophilic plastics are removed from the lower flotation apparatus part as the precipitate IV.

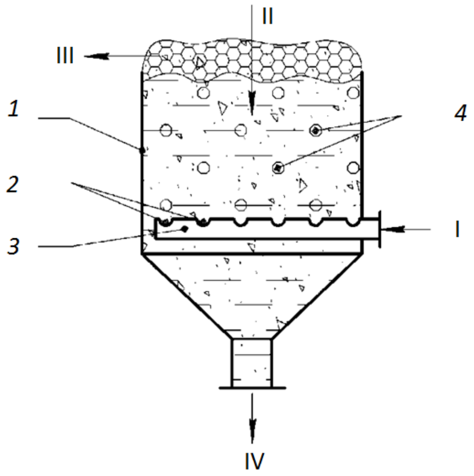

1 – the container; 2 – the holes of the aerator; 3 – the aerator; 4 – the air bubbles. The flows: I – supply of the air; II – supply of the mixture of milled plastics; III – discharge of the concentrate; IV – removal of the precipitate

Fig. 1. Scheme of the flotation apparatus with pneumatic aeration of the liquid

The promising flotation separation method of the mixture of milled plastics can be widely used in the production of plastic products, in the processing of industrial wastes, as well as in the separation of plastic wastes of household origin in plastic recycling plants. The flotation separation of the mixture of milled plastics according to the proposed process can be carried out in the batch or continuous mode.

To carry out subsequent theoretical and experimental studies of the proposed flotation separation method of the mixture of milled plastics, it is necessary to analyze factors affecting the flotation process.

The flotation is a complex set of subprocesses of a diverse nature, which are greatly influenced by the design and technological factors of the apparatus and process.

First, let's consider the design apparatus parameters (which are determined during its design). The *design* (shape) of the working zone is able to influence on the nature and direction of the phase flow in the apparatus volume, on the possibility of uniform aeration of the working liquid, on the presence of stagnant zones in which the material can become lodged and accumulate. The column apparatuses can be, for example, round, oval, square and other forms of cross-section with a constant or variable cross-section in height. The *area* of the column apparatus is a characteristic that determines its productivity, but at the same time it affects the working liquid aeration uniformity. The *height* of the liquid layer above the aerator (the column height) and *depth* (level) of the *material supply* determine the length of the path overcome by the particles of the separated materials and the gas bubbles, as well as the probability of the particle colliding with the bubble when they pass the working apparatus volume. Insufficient height of the aerated liquid reduces the probability of the particle colliding with the bubble when they pass through the working apparatus volume. And excess height of the aerated liquid increases the probability of destruction of the formed "bubble – particle" complexes, and also increases the hydraulic resistance when the air is supplied through the aerator. The *area* and *direction of the material flow* affect the uniformity of its distribution in the apparatus, the path length and the probability of collision with the bubbles. The *method of supplying the surfactant* and the *way it is mixed* in the working volume determine its consumption, since the more uniformly it is distributed in the working liquid, the more effectively it is used. The *method of selection of the foam and concentrate* (forced or self-flowing) determines the foam product motion mode and method of *organizing the liquid motion* in the apparatus, the presence of circulation. The gas bubbles distribution uniformity along the apparatus section is determined by the aerator design. The *aerator holes diameter and their number* are parameters that affect the bubbles' size, their number in the apparatus volume, and the gas speed in the hole.

The technological flotation process parameters include operating conditions of the phases and their physical properties. The operating conditions affecting the flotation process are *consumptions and supply of the phases, their motion speed, concentration of the surfactant, size and disperse phases relation, time of the process carrying out.*

The physical phase properties that generally affect the flotation process are *the liquid temperature, the gas and liquid viscosity, the phase densities, the particle parameters (size, shape, surface state), surface tension, type of the surfactant, chemical composition of the separated plastics, salt content, hydrogen index (acidity), the liquid pressure, the gas pressure in the bubble, partial pressure of the gas dissolved in the liquid, diffusion of the gas and surfactant* and other parameters [8].

Accounting for the effect of the physical phase properties on the flotation process is very complicated, since they can exert mutual influence on each other, and dependences of these influences cannot always be accurately determined. The operating conditions of such three-phase systems are also quite complex and require many simplifications and assumptions. All this complicates to analyze the research objects. Therefore, in the future it is necessary to choose which parameters and properties will be used to create and study the flotation separation process of polymer wastes.

Some parameters of the column apparatus can be selected using the data already available in the literature and general research methods (comparison, abstraction, analysis, analogy, synthesis, generalization). So, for example, among the whole variety of forms of the cross section of the column apparatus, the most practical is round shape, since it is easier to organize the uniform aeration of the working liquid [9]. In such column apparatuses, with the constant cross section in the height and the smallest number of structural elements, there are practically no stagnant zones in the internal volume in which the material can become lodged and accumulate. The feeder supplying the mixture of plastics to the apparatus should preferably have the smallest projection area on the plane of the apparatus cross section. As when the material enters the working liquid, its motion is directed downwards, then the material must be supplied in the upper apparatus part towards the ascending flow of the bubbles. This feeder arrangement contributes to a longer path length and greater probability of collision of the material particles with the bubbles. In order to distribute the supplied material evenly in the apparatus, it is advisable to place the feeder coaxially to it. However, the optimum supplying depth should be studied, since when supplying the material, the foam layer may have accidental involving (accidental removal) of the non-float component by the gas bubbles into the foam product, which will contaminate the concentrate.

There are several ways to select the foam product from the flotation liquid surface – forced (vacuum pumping, mechanical set-downs of various designs, etc.) or by gravity. In general case, it is necessary to carry out theoretical and experimental studies for each case. At that, it is necessary to compare the degree of spontaneous foam destruction during the time of the foam product presence over the liquid with the degree of the foam destruction under the influence of mechanical set-down and choose the optimal method for selecting the foam product. It should be noted that in the column flotation apparatuses, the presence time of the foam product over the liquid is small, that allows use the method of selecting the foam product by gravity. This method is the most economical, easy to manufacture and operate. The foam product is not subjected to mechanical influences and only can be spontaneously destructed (coalesced) depending on the physical properties of the materials and the presence time over the liquid. With this method, the liquid flows with the foam product over the edge of the flotation column and comes to the special launder. Such method for selecting the foam product involves continuous flow of the working liquid over the edge of the column, for which it is necessary to continuously supply the liquid to the column. The continuous liquid supply is also due to the need to maintain its certain level in the column. It is better to supply the liquid through the feeder of the initial mixture of milled plastics along with the particles of plastics, which will prevent them from sticking to the feeder walls, since the particles can come to the flotation wet, after preliminary washing.

The absence of a mechanical stirrer in the column flotation apparatus determines the way in which the surfactant is supplied into the working liquid flow, as in its turbulent motion in the pipeline and supply to the column, the necessary degree of mixing can be ensured. Let's hypothesize that the surfactant is uniformly distributed in the working liquid, and therefore the surfactant diffusion effect will be also neglected. Let's also hypothesize that the partial pressure and diffusion of the gas dissolved in the liquid have negligible effect on the flotation process [10]. There is no special external influence on the working medium (by ultrasound or electromagnetic field). The influence of salt content and hydrogen index was not taken into account (the quality of water used in the experiments corresponds to the quality of tap water for domestic needs).

Therefore, using the mathematical dependences, or experimentally, it is necessary to determine the following parameters of the flotation process and the apparatus design for its implementation: the air consumption, the height of the aerated liquid layer (the column height), the material supply depth, the liquid temperature, the surfactant concentration, the aerator design, the diameter of the aerator holes and their quantity.

CONCLUSION

Based on the analysis of the main methods of plastic waste separation, the method for the flotation separation of the mixture from milled plastics of various types based on the change in their hydrophilic property or hydrophobicity by supplying the surfactants and the gas bubbles into the working liquid into its working volume was proposed. The flotation apparatus design was proposed for this method.

The analysis of factors influencing the flotation process with consideration of the apparatus' design parameters, methods for feeding the surfactants, mixing, selection of the foam and concentrate, as well as technological parameters and physical properties of the phases, was carried out.

The list of the flotation process' parameters was determined, which must be specified using mathematical relations or experimentally.

REFERENCES

1 Enick R. The microsortation of post-consumer thermoplastics using near-critical liquids // Globec'96: 9PthP global environment technology congress together with Recycle'96: environmental technology. - Zurich, 1996. – P. 18–25.

2 Super M., Enick R.M., Beckman E.J. Separation of thermoplastics by density using near- and supercritical fluids as a precursor to recycling // ANTEC 91: in search of excellence: 49PthP annu. techn. conf. - Brookfield, 1991. – P. 2130–2133.

3 Super M.S., Enick R.M., Beckman E.J. Density-based separation of thermoplastics found in the postconsumer waste stream. Resources, Conservation Recycling, 1993, Vol. 9, No 1/2, Pages: 75–88.

4 Altland B.L. Optimization of the high-pressure, near-critical liquid based on microsortation of recyclable post-consumer plastic. Resources, Conservation Recycling, 1995, Vol. 15, No. 3/4, Pages: 203–217.

5 Serad G.A., Thornburg T.S. Separation of polyethylene terephthalate and polyvinyl chloride using supercritical carbon dioxide. Patent No US5462973A, 2017.

6 Kobler R.W. Polyvinyl chloride–polyethylene terephthalate separation process and product. Patent No US5234110A, 2017.

7 Fahrbach G., Schnettler H.R. New, dry preparation techniques to prepare used packaging plastics for feedstock recycling // Globec’96: 9PthP Global environment technology congress together with Recycle’96: Environmental technology. - Zurich, 1996. – P. 64–68.

8 S.S. Kutateladze, M.A. Styrikovich. *Gidrodinamika gazozhidkostnyx sistem* [Hydrodynamics of the gas-liquid systems.]. Moscow: E`nergiya, 1976, 296 p.

9 Yu.I. Rubinstein. *Pennaya separaciya i kolonnaya flotaciya* [Foam separation and column flotation]. Moscow: Nedra, 1989, 303 p.

10 I.O. Protodyakonov. *Gidrodinamika i massoobmen v sistemax gaz–zhidkost'* [Hydrodynamics and mass exchange in the systems gas]. Leningrad.: Science, 1990, 348 p.

IRSTI 61.13.21

CATALYSTS FOR THE HYDROGENATION OF FURFURAL

Duisembiyev M.Zh.*
L.N. Gumilev Eurasian National University, Astana, Kazakhstan
****Corresponding Author's Email:*** *m.duisenbiev@mail.ru*

ABSTRACT

The proposed invention improves the activity of the catalyst for the hydrogenation of furfural based nickel-aluminum leached alloy containing promoting additive. This is achieved by using as-promoting additives zirconium or niobium or molybdenum in an amount of 1.0-10.0 wt. % By weight of nickel. It was possible to increase the activity of Raney nickel (50% AI) catalyst THFA 1.5-1.8 times. Furthermore, the proposed catalysts can be regenerate and re-used in the hydrogenation of furfural. The catalyst for the hydrogenation of furfural based nickel-aluminum leached alloy containing promoter additive, characterized in that as-promoting additives alloy contains zirconium or niobium, or molybdenum in an amount of 1.0 – 10.0 wt. % By weight of nickel.

Keywords: hydrogenation of furfural , tetrahydrofurfuryl alcohol, aluminum- nickel catalyst.

INTRODUCTION

The growing demand for sustainable and environmentally friendly chemical processes has driven significant interest in the conversion of biomass-derived feedstocks into valuable chemicals and fuels. Among these feedstocks, furfural, a heterocyclic aldehyde derived from lignocellulosic biomass, has emerged as a key platform chemical due to its versatility and wide range of applications. One of the most important derivatives of furfural is furfuryl alcohol, a critical intermediate used in the production of resins, adhesives, and fine chemicals. The hydrogenation of furfural to furfuryl alcohol is a pivotal reaction in this context, as it enables the transformation of a renewable resource into industrially relevant products.

The hydrogenation of furfural is a catalytic process that typically involves the reduction of the carbonyl group (C=O) to a hydroxyl group (C-OH) using hydrogen gas (H_2) in the presence of a suitable catalyst. This reaction can proceed through various pathways, leading to different products such as furfuryl alcohol, tetrahydrofurfuryl alcohol, and even ring-saturated compounds, depending on the reaction conditions and catalyst properties. Achieving high selectivity toward furfuryl alcohol while minimizing the formation of undesired by-products is a major challenge in this process.

Catalysts play a central role in determining the efficiency, selectivity, and sustainability of the hydrogenation reaction. A wide range of catalytic systems, including noble metals (e.g., Pd, Pt, Ru), non-noble metals (e.g., Cu, Ni, Co), and bimetallic or supported catalysts, have been explored for this purpose. The choice of catalyst, along with reaction parameters such as temperature, pressure, and solvent, significantly influences the reaction kinetics and product distribution. Additionally, the development of robust and reusable catalysts is essential for the economic viability and environmental sustainability of the process.

This article focuses on the recent advancements in catalytic systems for the hydrogenation of furfural to furfuryl alcohol. It provides an overview of the different types of catalysts, their synthesis methods, and their performance in terms of activity, selectivity, and stability. Furthermore, the role of catalyst supports, promoters, and reaction conditions in optimizing the hydrogenation process is discussed. By addressing the challenges and opportunities in this field, this work aims to contribute to the development of efficient and sustainable catalytic processes for the valorization of biomass-derived compounds.

MATERIALS AND METHODS

Chemicals and Reagents: Furfural (purity ≥ 99%) was used as the primary feedstock for hydrogenation. Hydrogen gas (H_2, purity ≥ 99.9%) was employed as the reducing agent. Catalysts: Noble metal catalysts (e.g., Pd/C, Pt/Al_2O_3, Ru/C), non-noble metal catalysts (e.g., Cu-Cr-O, Ni/SiO_2, Co/Al_2O_3), and bimetallic catalysts (e.g., Cu-Ni, Pd-Fe) were used. Solvents: Isopropanol, ethanol, and water were used as reaction media. All chemicals were of analytical grade and used without further purification unless otherwise specified.

Methods

Catalyst Preparation: Supported Noble Metal Catalysts: Pd/C and Pt/Al_2O_3 catalysts were prepared by incipient wetness impregnation. The supports (activated carbon or alumina) were impregnated with aqueous solutions of palladium chloride ($PdCl_2$) or chloroplatinic acid (H_2PtCl_6), followed by drying at 110°C and reduction under hydrogen flow at 300°C for 2 hours. Non-Noble Metal Catalysts: Cu-Cr-O catalysts were synthesized by co-precipitation of copper(II) nitrate and chromium(III) nitrate solutions, followed by calcination at 400°C for 4 hours. Ni/SiO_2 and Co/Al_2O_3 catalysts were prepared by wet impregnation of nickel nitrate or cobalt nitrate on silica or alumina supports, followed by calcination and reduction. Bimetallic Catalysts: Cu-Ni and Pd-Fe catalysts were prepared by sequential impregnation or co-impregnation of metal precursors on suitable supports, followed by calcination and reduction.

Hydrogenation of Furfural: The hydrogenation reactions were conducted in a high-pressure batch reactor equipped with a temperature controller, pressure gauge, and magnetic stirrer. Furfural was dissolved in a selected solvent (e.g., isopropanol or water) and introduced into the reactor along with the catalyst. The reactor was purged with nitrogen to remove air, followed by pressurization with hydrogen to the desired pressure (10–50 bar). The reaction was carried out at temperatures ranging from 100°C to 200°C for 2–6 hours under continuous stirring.

Product Analysis: The reaction products were analyzed using gas chromatography (GC) equipped with a flame ionization detector (FID) and a capillary column (e.g., HP-5). The identification of furfuryl alcohol and other by-products (e.g., tetrahydrofurfuryl alcohol, furan, and ring-saturated compounds) was confirmed by gas chromatography-mass spectrometry (GC-MS). The conversion of furfural and the selectivity toward furfuryl alcohol were calculated based on the GC data.

Catalyst Characterization: The catalysts were characterized using various techniques to understand their structural and textural properties: X-ray diffraction (XRD): To determine the crystalline phases of the catalysts. Scanning electron microscopy (SEM): To analyze the surface morphology. Brunauer-Emmett-Teller (BET) analysis: To measure the specific surface area and pore size distribution. Temperature-programmed reduction (TPR): To study the reducibility of the catalysts. Transmission electron microscopy (TEM): To examine the dispersion of metal nanoparticles.

RESULTS AND DISCUSSION

The present invention relates to the manufacture of catalysts for the hydrogenation of furfural to tetrahydrofurfuryl alcohol (THFA).

However, this catalyst exhibits low activity in the hydrogenation of furfural in THFA, except that it is not recovered and discharged after a single use of the column and sent to the recovery of nickel.

The proposed invention provides a highly active catalyst nickel-aluminum rafting in the hydrogenation of furfural. This is achieved by the introduction of Ni - 50% Al alloy additions of zirconium or niobium or molybdenum in an amount of 1.0-10.0 wt. % [1].

Example. For the preparation of Ni-Al-Zr alloy composition (wt. %) in a quartz crucible 45-50-5,0 load 52g of aluminum in the form of pieces of 3-5 mm, then it melted at 1300-1400°C in the high right oven. In the resulting melt is injected 45g nickel and zirconium in the form of 5g pieces of 1-2mm. The temperature of the furnace was raised to 1700-1800°C and held in the melt for 5 minutes. Dale melt poured into graphite molds, cooled in air to room temperature, ground, sieved and leached with 20% aqueous sodium hydroxide solution in a boiling water bath for 2 hours, then poured caustic, and the catalyst is washed with water until neutral to phenolphthalein. Thus prepared catalyst is used for the hydrogenation of furfural,Activity of the catalysts were tested in an autoclave Vishnevsky cap. 250cmP^3 Pwith vigorous stirring of the reaction mixture. Hydrogenation using 10% aqueous solution of freshly distilled furfural and 0.5 g of the catalyst hydrogenation is carried out at a temperature of 90 and a hydrogen pressure of 4 MPa. Duration of the experiment is 60 minutes.

Separate samples of alloy catalysts were tested in a stationary mode, the pure furfural solvent-free installation on a solid column type in a known manner. The catalyst was prepared as follows: 195g minced alloy with an average particle diameter of 3-5mm, loaded into a special vessel, pour calculated of 10% aqueous sodium hydroxide solution and leached at room temperature at a certain depth (30-40%), controlled by the meter GSS-400. Leaching of aluminum calculated by known methods [2].

$$Al + NaOH + 3HR_2RO = Na\,[Al\,(OH)R_4R] + 1.5\ HR_2R \uparrow$$

After isolation of the equivalent amount of hydrogen from alkali catalyst washed with water until neutral to phenolphthalein. He was then charged into the reactor. Before the experiment, the catalyst was saturated with hydrogen at 120°C to the complete removal of water vapor.

The first leaching (30%) on aluminum conduct outside the reactor, and the subsequent (3-5%) - directly in the reactor with a 10% aqueous solution of sodium hydroxide 100P°PC

Floatable industrial Ni-Ti catalyst activates the same way.

Analysis of the products of hydrogenation of furfural carried by gas-liquid chromatography on a chromatograph "Chrome - 4" with flame ionization detector at the same time as the stationary phase using polyethylene glycol - 6000, inert solid support - hromaton with grains of 0,1-0,2 mm. Chromatographic conditions are as follows: Column temperature -

145°C , the column length - 2.4 m hydrogen consumption - 50cmP^{3}P/min, air flow - 300 cmP^{3}P/min and flow of argon - 100-200 cmP^{3}P/min; current sensitivity - 50 • 10 P^{-10}PA.The activity of the suspended catalyst is judged by the reaction rate (W), expressed in grams per 1 g of furfural converted catalyst for 0.5 h (g / g 0.5 h).

The activity of the catalysts stationary inferred from the magnitude of the contact load, expressed in liters per 1 liter of the substance hydrogenated catalyst for 1 h (l/l•Cat • h or hP^{-1}P), corresponding to 98-100% yield of the desired product [2].

Table 1 shows the results of hydrogenation of furfural at 90°C and 4 MPa on glass nickel (50% Al) alloy catalysts with additions of zirconium and niobium, and molybdenum. It can be seen that the hydrogenation of furfural in the studied catalysts are selectively with simultaneous formation of furfuryl (FA) dihidrofurfuril (DHFA) alcohols and THFA. The maximum yields of intermediate FA and DHFA respectively 40-42 and 6-8%. Exit THFA 20 min. hydrogenation grows slowly and then rapidly increases and reaches 43-52% in 60 min. Process, depending on the nature of the modifying metals. The total yield of the reaction products is increasing continuously and 60 minutes. Process reaches 92-98%. Activity modified catalysts is 1,5 – 1,8 times higher than the skeletal Ni (50% Al) or without the addition of 1.8-2.0 times higher than the industry Ni-Ti contact number of activity greatest show alloy Ni-Mo catalysts. Investigated catalysts increase in activity arranged in a row: Ni - Zr<Ni-Nb<Ni-Mo.

Results of the continuous hydrogenation of furfural on stationary nickel catalysts are shown in Table 1.

Table 1 - Results of the continuous hydrogenation of furfural on nickel catalysts

The degree of leaching Al, %	t, P$^{\circ}$PC	PR$_{H2}$R, MPa	WR$_{H2}$R, hP^{-1}	WR$_{ff}$R, hP^{-1}	The yield of products		The relative duration of the process, h
					FA	THFA	
1. Ni-50% Al-5% Zr							
30	80-160	4	180	0.42-0.62	0.0-2.0	98-100	424
35	90	2-6	180	0.41-0.60	0.0-1.0	99-100	420
40	80	4	100-180	0.43-0.65	0.0-1.5	98.5-100	410
2. Ni-50% Al-5% Nb							
30	80-160	4	180	0.44-0.64	0.0-1.0	99-100	444
35	80	2-6	180	0.42-0.63	0.0-2.0	98-100	440
40	80	4	10-180	0.43-0.65	0.0-2.0	98-100	435
3. Ni-50% Al-5% Mo							
30	80-160	4	180	0.46-0.65	0.0-2.0	98-100	450
35	80	2-6	180	0.44-0.64	0.0-1.0	99-100	445
40	80	4	10-180	0.43-0.63	0.0-1.8	98.2-100	440
4. Ni -50% Al 2.8% Ti							
30	80-160	4	180	0.37-0.58	0.0-2.0	98-100	398

Table 1 shows that the main product of the hydrogenation of furfural in the studied catalysts is THFA whose output reaches 98-100%. Activity and stability of the investigated stationary nickel catalysts 1.1-1.24 times higher than that of commercial Ni-Ti contact [2].

CONCLUSION

Increasing the experimental temperature from 80 to 160°C, the hydrogen pressure - in the range of 2-6 MPa hydrogen bubbling rate from 10 to 180 hP^{-1}P has a positive effect on the speed of the continuous hydrogenation of furfural on stationary nickel catalysts.

It should be noted, one hundred proposed alloy nickel catalysts with the addition of zirconium or niobium or molybdenum in contrast to the well-known Ni-2,8% Ti catalyst is easily leached, washed from alkali, more selective and stable. In addition the proposed catalysts can be recovered and reused in the process of hydrogenation of furfural.

REFERENCES

1 Duisembiyev M.Zh. Hydrogenation furfurily in furfural alcohol in presence of floatable catalyst //The materials of international conference "The development of science in modern era". –Kiev, 2012. - P.17-20.

2 Duisembiyev M.Zh. The finding and development of catalyst of hydrogenation of furfural// The materials of international conference. - Novosibirsk, 2012. - P.171-175

3 Achieving Product Control in Furfural Hydrogenation Using Intermetallic Catalysts. Available from: http://dx.doi.org/10.1021/acscatal.4c04091.s001

4 Stewart MM. Some metallic oxides as promoters for copper oxide catalysts in the hydrogenation of furfural. Available from: http://dx.doi.org/10.31274/rtd-180813-16330

5 Thompson ST, Lamb HH. Alloying and Segregation in PdRe/Al2O3 Bimetallic Catalysts for Selective Hydrogenation of Furfural. Catalysts [Internet]. 2024 Sep 7;14(9):604. Available from: http://dx.doi.org/10.3390/catal14090604

6 Wang Y, Zhao D, Rodríguez-Padrón D, Len C. Recent Advances in Catalytic Hydrogenation of Furfural. Catalysts [Internet]. 2019 Sep 24;9(10):796. Available from: http://dx.doi.org/10.3390/catal9100796

7 Kuhaudomlap S. Preparation of nickel phyllosilicate catalysts by one-step modified spherical silica synthesis in carbon dioxide hydrogenation and selective hydrogenation of furfural to furfuryl alcohol. Available from: http://dx.doi.org/10.58837/chula.the.2021.54

8 Supported Palladium Catalysts for the Selective Hydrogenation of Furfural with Polymethylhydrosiloxane. Available from: http://dx.doi.org/10.1021/acssuschemeng.4c06333.s001

9 Selective Hydrogenation of Furfural to Tetrahydrofurfuryl Alcohol Using Supported NickelCobalt Catalysts. Available from: http://dx.doi.org/10.1021/acs.iecr.9b01443.s001

10 Byun MY, Park DW, Lee MS. Effect of Oxide Supports on the Activity of Pd Based Catalysts for Furfural Hydrogenation. Catalysts [Internet]. 2020 Jul 24;10(8):837. Available from: http://dx.doi.org/10.3390/catal10080837

11 Wonglekha K. Effects Of Tio2 Support And Co Addition On Ni/Tio2 Catalysts In Selective Hydrogenation Of Furfural To Furfuryl Alcohol. Available from: http://dx.doi.org/10.58837/chula.the.2018.52

12 Bardestani R, Biriaei R, Kaliaguine S. Hydrogenation of Furfural to Furfuryl Alcohol over Ru Particles Supported on Mildly Oxidized Biochar. Catalysts [Internet]. 2020 Aug 13;10(8):934. Available from: http://dx.doi.org/10.3390/catal10080934

IRSTI 06.75.02

ECONOMIC SECURITY OF ENTERPRISES A KEY COMPONENT FOR THE SUCCESS OF MODERN SMALL BUSINESSES

Aidarova A.B.*, Bitemirov B.T.
M. Auezov South Kazakhstan University, Shymkent, Kazakhstan
****Corresponding Author's Email:*** ab_moon@mail.ru

ABSTRACT

In the context of ongoing global economic instability, the development and implementation of effective systems for ensuring the economic security of enterprises has become one of the most pressing challenges for both science and practice. Businesses are increasingly compelled to adapt to political and socio-economic turbulence, identify suitable solutions to complex problems, and mitigate the risks that threaten their operations.

This article examines the concept of economic security at the enterprise level, outlining the primary threats that affect its functionality. It provides an evaluation of the factors that determine the level of economic security within an organization. The authors introduce a classification of the functional components of economic security and explore their interrelations with strategies for safeguarding enterprises. The analysis highlights how these functional components can serve as the foundation for developing comprehensive measures aimed at countering potential threats and enhancing the enterprise's overall economic security. By doing so, these measures can bolster the organization's adaptability to changes in the business environment, ensuring stable operations and fostering long-term development.

The implementation of strategies designed to ensure the economic security of an enterprise will not only contribute to its stability but also improve the efficiency of its financial and economic activities. Furthermore, these strategies will play a key role in enhancing the economic potential of Kazakhstan's industrial sector and, more broadly, in strengthening the national economy.

Keywords: economic security, enterprise, threat, protection, danger, counteraction

INTRODUCTION

For an extended period, society has grappled with the challenge of ensuring economic security at all levels. Countries worldwide have strived to establish stable economic development both at the national level and within individual enterprises. The importance of targeted actions aimed at safeguarding the economic security of enterprises has become particularly evident in the face of the current crisis and ongoing processes of national modernization [1].

The economic security of an enterprise refers to a state of stability in which the organization is protected from the adverse effects of both external and internal threats, as well as destabilizing factors. This security ensures the consistent achievement of the enterprise's core commercial objectives and statutory goals.

In general, the economic security of an enterprise encompasses:

− high financial efficiency, independence and sustainability of the enterprise;
− development and competitiveness of the technological base of the enterprise;
− high level of organization of enterprise management;
− strict personnel selection;
− ensuring compliance with environmental standards;
− an effective mechanism for legal regulation of all areas of the enterprise's activities; ensuring information security of the enterprise;
− guarantees of the safety of the enterprise's employees, as well as the safety of their property and professional interests [2].

At various stages of its development, every enterprise encounters the challenge of safeguarding its interests against illegal actions by competitors and malicious external threats. In the context of today's often unregulated competitive environment, the inadequacies of current legislation, the arbitrary actions of fiscal authorities, and other destabilizing factors, it becomes imperativeeven during the initial stages of business formation (such as the drafting of a business plan and charter)to implement measures ensuring the enterprise’s economic security. These measures are crucial for preventing or mitigating the negative effects of both external and internal threats.

MATERIALS AND METHODS

The methodological foundation is based on the theoretical concepts and practical contributions of both domestic and international scholars on the subject, as well as materials from scientific conferences.

RESULTS AND DISCUSSION

Each enterprise is engaged in specific economic and commercial activities, meaning that the concepts of "external" and "internal" threats will vary depending on the nature of the organization.

Common external threats and destabilizing factors include: illegal activities by criminal organizations, competitors, and individuals—such as racketeering, expropriation, and blackmail. Enterprises may also encounter industrial espionage or fraud. Other threats include dealing with insolvent or irresponsible business partners, former employees dismissed for misconduct, and illegal actions by corrupt officials within regulatory and law enforcement agencies.

Internal threats and destabilizing factors commonly arise from the actions or inactions (both intentional and unintentional) of the company’s employees, which may harm the organization’s interests and result in economic damage. Additional threats include the leakage or loss of competitive information resources, including commercial secrets or confidential data; damage to the company's business image and reputation within the community; problems in relationships with current or potential partners and clients; conflicts with competitors, regulatory bodies, or representatives of the criminal underworld; and incidents of industrial injury or employee fatalities [3].

The current state of the Kazakh economy underscores the necessity of establishing a comprehensive system for the economic security of businesses. Such a system would safeguard the vital interests of individuals and legal entities. Economic security, in this context, refers to the protection of the enterprise’s scientific, technological, production, and human resources from both direct (active) and indirect (passive) economic threats.

The economic security of an enterprise refers to the optimal utilization of corporate resources to prevent potential threats and ensure the stable operation of the organization both in the present and in the future.

For industrial enterprises, assessing economic security is particularly crucial, as their active potential serves as a key stabilizing factor in times of crisis, acting as a guarantor of economic growth and the preservation of national economic independence and security. The challenge of ensuring economic security is relevant to every enterprise, regardless of its industry or market focus. This challenge arises not only during times of crisis but also while operating within a stable economic environment.

In modern conditions, the process of successful functioning and economic development of Russian enterprises largely depends on the improvement of their activities in the field of economic security. As the main factors that negatively affect the safety of business activity in the Republic of Kazakhstan, the following can be distinguished:

- active involvement of government representatives and administrators in commercial activities;
- utilization of criminal organizations to exert influence over competitors;
- lack of comprehensive legislation to effectively counteract unfair competition;
- unfavorable conditions for conducting scientific and technological research in the country;
- lack of detailed and objective information about business entities and their general financial situation;
- insufficient business culture within the corporate environment;
- the use of operational and technical methods to gather competitive intelligence [4].

It should be emphasized that not all enterprise managers are fully aware of the necessity to establish a reliable economic security system. The Law of the Republic of Kazakhstan "On National Security of the Republic of Kazakhstan" defines "security" as the state of protection of vital interests [5].

However, there remains a pervasive stereotype that this domain falls solely under the purview of the state and specialized agencies. This misconception is at the root of the inadequate understanding of these issues, particularly among top-level managers of enterprises and organizations. Determining the specific actions required to safeguard critical resources is often a challenging task. Consequently, many managers focus primarily on establishing security structures within the enterprise while largely overlooking organizational-technical, legal methods, and information protection strategies.

As a result, for instance, issues concerning the protection of commercial secrets are frequently neglected in licensing agreements and contracts for the creation of scientific and technical products, leading to the potential leakage of commercially sensitive information [6].

Information security measures for individual enterprises can vary in scale and form, depending on the enterprise’s production, financial, and other capabilities, as well as the quantity and sensitivity of the information that needs protection. At the same time, the selection of these measures should be based on the principle of reasonable adequacy, adhering to a balanced approach in financial decisions. Excessive information protection, as well as negligence in safeguarding it, can result in lost profits or significant financial losses.

Thus, the economic security project of an enterprise constitutes a unified organizational and technical system. During its formation, the concept or policy of security is developed, which includes a set of mandatory measures designed to create a comprehensive action plan for protecting the enterprise. This plan involves determining the structure of the security service (SS), its position within the organizational framework, its sphere of authority, rights, and powers, as well as establishing protocols for action in various situations to prevent conflicts between departments. A common issue is that many individuals perceive the requirements of the SS as overly stringent. However, adherence to these principles will either prevent such conflicts or allow them to be resolved quickly and effectively.

The economic security policy outlines the proper use of communication and computing resources from an organizational perspective, establishes rules for access to protected information, sets guidelines for handling confidential data, and details procedures for preventing and responding to security breaches.

It is important to emphasize that the effectiveness of a security policy can only be achieved when its implementation is the result of collaborative efforts among the organization’s employees, who must fully understand its various aspects, and the managers, who must have the authority to ensure its enforcement. An equally crucial factor in the success of the security policy is the readiness of personnel to comply with its requirements, ensuring that each obligation related to maintaining the security regime is met. Compliance with the policy should be ensured through the appointment of a responsible individual for each specific issue.

Naturally, the key provisions of the security policy must be codified in the relevant regulatory documents, the content and structure of which will depend on the specific nature of the organization. However, in most cases, no enterprise can function without policies covering commercial secrecy, information protection, security network administration, rules governing access to information within automated systems, regulations for admitting personnel and visitors to areas where critical information processing occurs, and procedures for conducting official investigations into violations of safety protocols.

Efforts to equip and support the activities of the information security system (ISS), along with the creation of a comprehensive system of administrative documentation, are part of an organizational framework that helps achieve a high level of information security. However, these measures alone are insufficient to maintain the security system at an optimal level without implementing a series of additional organizational and technical measures. Although the full range of these measures is too extensive to list in detail within this article, it can be said that they enable the timely identification of new information leakage channels, the implementation of countermeasures to neutralize them, the enhancement of the security system, and the swift response to security breaches [7].

The developed documents outline the necessary functions for organizing the work of the security service (SS), as well as the control, verification, and other specialized tasks it performs in its operations. The main functions include:

− administrative and managerial – preparation of decisions regarding the maintenance of security and confidentiality regimes, determination of the provisions, rights, obligations, and responsibilities of officials on safety matters, and the representation of the enterprise in this area of activity;

− economic and administrative – identification (in collaboration with other divisions of the enterprise) of the resources required to address the enterprise's security needs, and the preparation and implementation of organizational, technical, and legal measures aimed at protecting its assets, including intellectual property;

− accounting and control – identification of critical areas in financial, economic, production, commercial, and other activities that require protection; analysis of potential information leakage channels and other threats to the enterprise's financial stability and sustainability; assessment of their sources and establishment of effective control mechanisms;

− organizational and technical – creation of the organizational structure of the SS and other specialized units (e.g., information protection, economic security); facilitation of interaction between various departments to achieve the goals of the security policy;

− planning and production – development of comprehensive programs and specific plans to ensure the safety of the enterprise, along with the preparation and execution of corresponding measures.;

− material and technical – provision of material, technical, and technological support for the SS's activities, including equipping it with specialized tools;

− scientific and methodological – accumulation and dissemination of best practices in the field of security; organization of employee training in other divisions as necessary;

− informational and analytical – collection, processing, and analysis of data related to security, as well as the development and use of technical and methodological tools to support these activities [8].

Nevertheless, it is important to remember that equipping the SS with reliable tools, effectively prioritizing its activities, and executing any skilled work requires the involvement of specialists with the appropriate professional training and, equally important, significant practical experience in the field. The enterprise's security system must be designed by professionals, and collaboration with them can only be truly productive if it is based on long-term engagement.

CONCLUSION

The transition to market-based economies requires enterprise leaders not only to develop market strategies but also to implement a robust security strategy. This strategy should encompass specific programs aimed at protecting intellectual property and ensuring overall economic security. As a result, the role of the unit responsible for executing these tasks becomes crucial. This unit is tasked with ensuring compliance with security policies and protection plans, managing security measures, monitoring their proper functioning, detecting attempts or incidents of security breaches, and taking appropriate countermeasures.

The integrity of any component of an enterprise's infrastructure directly impacts its overall security. Consequently, the management process of the enterprise is inherently linked to security concerns.

REFERENCES

1 Belokur V.V. Ugrozy jekonomicheskoj bezopasnosti predprijatija: uchebnik / pod red. V.V. Belokura. – M., 2010. 135s.
2 Gaponenko V.F. Jekonomicheskaja bezopasnost' predprijatij. Podhody i principy [Tekst] / V.F. Gaponenko, A.A. Bespal'ko, A.S. Vlaskov.- M.: Os'-89, 2007. - 208 s.
3 3. Grunin, O.A. Jekonomicheskaja bezopasnost' organizacii / O.A.Grunin, S.A.Grunin. −SPb.: Piter, 2002. −160s.
4 Gusev, V.S. Jekonomika i organizacija bezopasnosti hozjajstvujushhih sub#ektov [Tekst] / V.S. Gusev i dr. - SPb.: Piter, 2004. 256s.
5 O nacional'noj bezopasnosti Respubliki Kazahstan. Zakon Respubliki Kazahstan ot 6 janvarja 2012 goda № 527-IV.
6 Donec L.I., Vashhenko N.V. Jekonomicheskaja bezopasnost' predprijatija: Uchebnoe posobie. - K.: Centr uchebnoj literatury, 2008. 240s.
7 Senchagov V.K. Jekonomicheskaja bezopasnost' Rossii. M., 2010. 815s.
8 Sudoplatov A.P. i dr. Bezopasnost' predprinimatel'skoj dejatel'nosti. M., 2008. 381s.

IRSTI 06.71.03

MAIN DIRECTIONS OF MODERNIZATION OF THE MANUFACTURING INDUSTRY OF THE REPUBLIC OF KAZAKHSTAN

Aidarova A.B.[*], Alimbay B.Zh.
M. Auezov South Kazakhstan University, Shymkent, Kazakhstan
[*]***Corresponding author's e-mail:*** ab_moon@mail.ru

ABSTRACT

The objective of this article was to explore the key directions of modernization within the structures of the processing industry in Kazakhstan's economy and to examine the foundational principles of its application in the development of the domestic processing sector.

Industrial modernization is a multifaceted process involving interconnected and interdependent components, where changes in certain elements lead to modifications in others, both quantitatively and qualitatively.

This article discusses the priority directions for the modernization of the processing industry, highlighting the essential characteristics of the modernization process. It also analyzes a range of measures for innovative and technological modernization and recommends focusing on these areas during the implementation of modernization efforts in Kazakhstan's processing industry.

For Kazakhstan, industrialization should be pursued through novel approaches that will facilitate the modernization and digitization of domestic enterprises, particularly those producing export-oriented products. This will contribute to the realization of long-term strategic objectives.

Industrial and innovative development is positioned as a primary priority for the country's economic and social advancement, serving as a critical factor in enhancing product quality and boosting the competitiveness of industrial production.

Keywords: industry, manufacturing industry, modernization, productivity, innovative activity, structure

INTRODUCTION

Currently, a critical factor for economic growth is the effective utilization of industrial potential, which enables the advancement of the entire national economy to a new technological level. The world is transitioning into the era of the "Industry 4.0" revolution, marked by rapid technological, economic, and social transformations.

This shift presents both challenges and opportunities for countries worldwide. As a result, the development of industry and its processing sector has become increasingly relevant, as it plays a crucial role in significantly enhancing labor productivity, both in theory and practice [1].

Global experience underscores that industrial and innovative development is a primary priority for the economic and social advancement of any nation. It is also a vital condition for improving product quality and enhancing the competitiveness of industrial production. Notably, private investment in research and development (R&D) constitutes approximately 90% of the global economy, ensuring a steady rise in the level of innovative development across economies.

When examining the issues of industrial modernization in Kazakhstan's economy, it is crucial to recognize that these processes involve not only the development of the entire industrial sector but also the advanced growth of the manufacturing sector.

Kazakhstan has the potential to achieve stable economic growth and a high technological level through the development of its manufacturing industry, thereby fostering a revival of innovative activity.

However, despite the initiatives and programs implemented by the government to promote the manufacturing sector, the structure of industrial production in Kazakhstan is still dominated by extractive industries, with insufficient growth in high-tech industries. Currently, industry constitutes approximately one-third of Kazakhstan's economic structure. The mining sector accounts for about 2.9% of employment and 18% of total value added. In terms of fixed capital investments, the manufacturing industry represents only 20.6% of the total.

In 2023, the manufacturing industry's contribution to Kazakhstan's GDP will be just 12.2%, with this decline primarily attributed to the growth of the service sector. Similar trends are observed in both developed and developing nations. In Kazakhstan, per capita exports of manufacturing products are two times lower than in Russia. While industrialization is gradually shifting focus towards manufacturing, the development level of this sector remains relatively low [2].

Furthermore, both the national economy as a whole and the manufacturing industry, in particular, are marked by high levels of moral and physical depreciation of the material and technical base, which contributes to the low competitiveness of many types of manufactured products. Additionally, the underdeveloped institutional environment, which hinders the effective utilization of scientific and technological achievements in production, has a detrimental effect on the development of the manufacturing industry in the country. This is particularly evident in the poor implementation of the commercialization of scientific developments. Therefore, it is imperative to improve the current structure of domestic industry and establish a new model that is tailored to Kazakhstan’s specific conditions.

Increasing the share of the manufacturing sector in Kazakhstan's economy and ensuring its sustainable development can be achieved through the implementation of key directions for structural modernization. To ensure the effectiveness of this process, it is crucial to identify problem areas where minimal efficiency is achieved from available resources and to establish the criteria and main parameters for optimizing operations. In this context, the government should create favorable conditions for the transition of the most efficient industrial sectors toward innovative development.

The application of effective methods and organizational forms of structural measures can positively impact qualitative changes within the economy, particularly in its technical, organizational, technological, and managerial components.

Thus, the primary objectives of modernization involve creating optimal conditions for the formation of a balanced economic structure, including a manufacturing sector that meets both technological and economic requirements, as well as enhancing the economic potential of high-tech industries [3]. For Kazakhstan, industrialization should be carried out using innovative approaches that will aid in modernizing and digitizing domestic enterprises, particularly those focused on export-oriented products, and thereby facilitate the implementation of long-term strategic plans.

In conclusion, the examination of the problem of modernization within the manufacturing industry and the identification of potential solutions underscore the relevance and importance of conducting such a study.

The theoretical aspects of structural modernization in industry are rooted in the historical progression of industrial revolutions, each driven by technological advancements that led to paradigm shifts. These technological leaps, which have been subsequently labeled as "industrial revolutions," include the intensive use of electricity (the so-called 2nd Industrial Revolution) and the widespread adoption of digitalization.

The three preceding industrial revolutions were triggered by significant technical innovations. The first industrial revolution, in the late 18th century, was fueled by the introduction of water and steam power. The second, occurring in the early 20th century, was characterized by the division of labor. The third, beginning in the 1970s, saw the introduction of automation technologies in production processes.

Currently, a wide range of studies exist on this topic, drawing upon the foundational works of industrial development theorists such as J.A. Schumpeter and N.A. Kondratiev. In addition to these classical figures, several prominent Russian scholars have contributed to the field, including A.V. Babkin, A.I. Tatarkin, L.V. Krasnyuk, and S.V. Kuznetsov. Their research, often focused on sectoral and regional levels, has highlighted various issues related to the structural, innovative, technological, and cluster aspects of industrial development [4].

To fully capture the essence of the structure of the manufacturing industry, it is essential to clarify key concepts such as "structure," "industrial structure," "optimal structure," "effective structure," and "industrial policy."

The term "structure" of an economic object is generally understood as the division of the object into components based on specific characteristics, with the establishment of relationships between these components that reflect the internal nature of the object. Furthermore, each subsystem that constitutes an economic object or category can be viewed as a separate system with its own structural elements.

In a narrower sense, "structure" refers to the system of reproduction of the total social product, consisting of various economic elements. Industry, as part of the broader economic system, can be considered within the framework of the economic structure. In this context, the term "industrial structure" can be defined as the set of internal relationships between the main elements of industry.

The optimal structure is understood as the best possible configuration among all available alternatives.

The concept of "industrial policy" has been defined by Harvard University Professor D. Rodrick as a policy aimed at stimulating specific types of economic activities and facilitating structural changes [5].

German researcher T. Altenburg, in his analysis of Western economists' interpretations, concludes that the vast majority of definitions of "industrial policy" encompass any government measures or a set of actions intended to either promote or prevent structural changes. From the Western perspective, industrial policy refers to state measures that enhance the structure of the economy through appropriate structural changes. In our view, "industrial policy" should be understood as a set of government actions designed to alter the structure of the economy by creating more favorable conditions for the development of specific (priority) sectors and industries [6].

The concept of "modernization" in a broader sense refers to the acknowledgment of economic, technological, and institutional backwardness, and the recognition that radical changes are required to facilitate the transition to a new stage of civilizational development. The theory of modernization, which involves updating and transforming an object in line with new technical conditions, emerged in the mid-20th century, when many newly independent nations in the Third World sought their own development models. For these countries, modernization represented the shift from traditional to modern societies.

The process of modernization began during the first industrial revolution, which marks the initial stage of this transformative journey. The second stage of modernization is linked to the development of an information society, driven by knowledge. In the context of industry, modernization can be viewed as reindustrialization, grounded in innovation and advanced technologies. This process involves increasing the share of science-intensive industries within the structure of production and exports through diversification, and overcoming the dominance of a one-sided raw material-based economy.

Diversification, which shifts the focus from raw material exports to an innovative economy, is considered the most optimal path for modernization [7].

For Kazakhstan, the modernization and diversification of the national economy, with a particular emphasis on boosting the share of the manufacturing industry, remains a priority. This is due to the objective factors that contribute to the inefficiency of the current economic structure.

MATERIALS AND METHODS

The research applied modern methods, including abstract-logical reasoning, systemic analysis, comparative analysis, economic statistical methods, causal analysis, classification, grouping, and scenario forecasting techniques, to determine the possible development options of the object.

RESULTS AND DISCUSSION

Main directions of industrial modernization.As outlined earlier, the primary objectives of modernizing the manufacturing sectors of Kazakhstan’s economy include achieving a higher level of integration into global economic relations, particularly in the fields of production, trade in goods and services, international finance, and the use of scientific, technical, and informational resources.

The modernization of the economy, and specifically its industrial structure, involves transitioning to a higher level of utilization of domestic progressive scientific and technical innovations in production. Therefore, it is crucial to modernize the material and technical base across all sectors of Kazakhstan’s economy, including mechanical engineering, metalworking, food production, light industry, and other industries. In addition, it is essential to create conditions for the training and retraining of highly skilled personnel capable of using the latest technology in all areas of activity. These efforts will contribute to the growth of science in Kazakhstan, which serves as the foundation for scientific and technological progress.

These objectives can be achieved through the development and implementation of a national industrial policy that establishes adequate institutional conditions for attracting investments and stimulating the growth of high-tech sectors of the manufacturing industry, particularly those producing competitive products for global markets.

The ability of the industrial structure to respond flexibly and appropriately to internal and external changes is crucial for its effective functioning. Modernization efforts should focus on developing an industrial structure capable of evolving into an organic and unified system that promotes rapid growth and expansion of the domestic market while also ensuring the global competitiveness of its products.

Progressive industrial changes can be implemented by considering the following conditions:

- macroeconomic and social stability;
- availability of natural resources;
- sufficient degree of development of the scientific and technical sphere;
- availability of qualified personnel that meet the requirements of "Industry 4.0" and a stable system of their training;
- regional features of the deployment of productive forces;
- historical and national features of industrial development.

An important factor in addressing the challenges of structural transformation is investment. The lack of capital investment has a detrimental impact on the comprehensive modernization of industry.

As demonstrated by the experience of foreign countries, continuous focus on improving technology and products is far more critical than simply emphasizing "technological achievements" alone [8].

The process of industrial modernization involves multiple interconnected and interdependent areas and elements, where both quantitative and qualitative changes in one aspect can lead to shifts in others. These reforms help maintain the integrity of the system while simultaneously enhancing its overall performance.

Improving the organizational structure of management for Kazakhstan's economy is a highly complex and labor-intensive task.

However, it is essential for achieving strategic goals and fostering cooperation, coordination, and control over business processes and resources. The core of this challenge lies in selecting an appropriate organizational structure that, when informed by organizational theory, can effectively interact with the external environment, allocate and direct financial and labor resources productively, and ultimately achieve the desired strategic objectives.

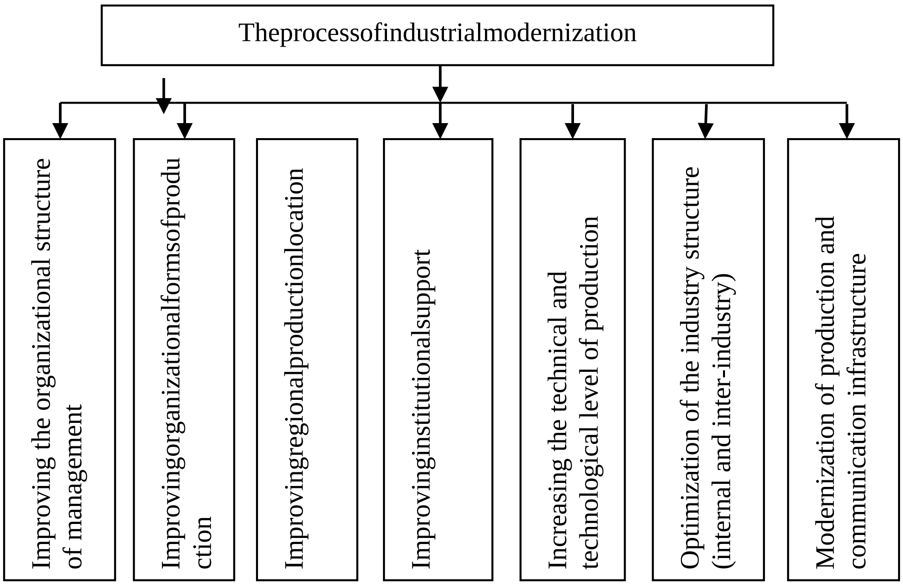

Fig. 1. Main directions of industrial modernization

Improving organizational forms of production. The enhancement of organizational forms of production is essential for the efficient functioning of the economy. This involves increasing the scale of public production, streamlining inter-industry, intra-industry, and territorial relations, and rapidly incorporating scientific and technological advances. In combination with addressing major socio-economic tasks, these factors create an objective need to improve organizational forms and management systems across all industries and production stages.

Improving the territorial location of production. The optimal location of enterprises within a country depends on the specific nature of the activities and the availability of key production factors. An important consideration in this context is assessing the efficiency of the use of natural, industrial, and human capital, as well as continuous production processes within the economic system.

Improving the territorial organization of production, coupled with a shift in the economic development model, diversification of regional innovation systems, and the development of transport, logistics, and communication infrastructure, fosters the emergence of new approaches and directions in the territorial division of the production structure. These changes help optimize the location of production units, ultimately contributing to the efficient use of resources and enhancing overall productivity.

Increasing the technical and technological level of production. A key aspect of industrial modernization, driven by the implementation of industrial policy measures, is the transition to innovative and digital technologies. This involves systematically introducing new technologies, modernizing outdated equipment, and continuously advancing the technical level of production. Achieving this requires the automation and mechanization of all technological processes, with careful consideration of the necessary material, labor, and financial resources. By fostering technological upgrades, industries can improve efficiency, reduce operational costs, and remain competitive in the global market.

Optimization of the sectoral structure (internal and inter-sectoral). The optimization of the sectoral structure within a region's economy is essential for establishing the relationships and interdependencies between sectors that will enhance the competitiveness of the region's economy.

In this context, the competitiveness of the regional economy refers to its capacity for sustainable socio-economic development, achieved through the effective utilization of its competitive advantages. These advantages include access to natural resources, skilled labor, scientific and managerial potential, a robust production base, and a conducive business climate. Additionally, the quality of managerial capabilities, infrastructure, and regional policies plays a crucial role in supporting competitiveness and fostering long-term economic growth. By optimizing sectoral relationships, regions can better leverage their strengths, drive innovation, and attract investments that contribute to overall economic prosperity.

Modernization of production andcommunication infrastructure. Production infrastructure plays a pivotal role in establishing and maintaining stable connections between economic entities, making its development, expansion, and modernization essential for enhancing production efficiency. By improving infrastructure, industries can benefit from more seamless interactions, optimized processes, and overall better coordination, all of which contribute to a more productive and competitive economy.

The modernization of communication infrastructure is equally critical, as it supports the internal needs of the country. This involves creating a robust communication network and upgrading communication facilities to ensure smooth and effective transmission of information across various sectors. Such modernization facilitates the movement of production factors and accelerates the exchange of information, which is crucial for business operations.

Furthermore, the evolution of communication infrastructure is not only a catalyst for enhanced connectivity but also a foundational element for the development of a digital economy. As the world becomes increasingly interconnected, the modernization of communication networks is essential to supporting digital transformation, enabling data-driven decision-making, and facilitating the growth of new technologies and industries..

Improving institutional support. The institutional approach to assessing trends associated with the innovative development of economic systems is particularly promising, as the speed and effectiveness of national economic growth largely depend on the dynamics of innovation. Institutionalism is vital because it offers a more nuanced understanding of the conditions, causes, and driving forces behind economic innovation, compared to traditional economic theories. This approach emphasizes that the pace of economic development is not solely determined by technological advancements or capital, but also by the institutional frameworks that govern innovation and its application within the economy.

The revitalization of innovative activity is essential for the continued qualitative and quantitative growth of the national economy. A robust institutional framework is crucial for fostering an environment conducive to innovation, which can spur new industries, improve productivity, and ultimately increase global competitiveness.

In this context, developing institutional aspects related to creating an innovative climate within economic organizations becomes a key factor in driving long-term economic progress. A well-structured institutional support system helps businesses and industries adapt to new technologies, encourages research and development, and ensures that innovation can be effectively integrated into various sectors.

While many economists link industrial reforms with sectoral changes, this perspective offers a limited understanding of the broader and more complex process of industrial modernization. Modernization involves not only shifts within specific industries but also changes in the institutional, technological, and regulatory frameworks that underpin the entire industrial structure. As such, industrial reforms must be viewed as part of a larger, multidimensional transformation that encompasses technological, organizational, and institutional innovations.

The content of this process is presented in Table 1.

Table 1 –Main characteristics of the modernization process

Characteristics of the process	Definition
comprehensive	It is formed by the systemic nature of modernization, in which a shift in one link of a structural chain affects structural changes in its other links.
continuity	The industrial complex is determined by the mobility and dynamism of its operating environment.
goal-orientedness	Determined by the main directives and the purpose of modernization activities. Modernization of the organizational structure of industry is understood as determining the best relationship and connections between small, medium and large economic entities, that is, establishing the most optimal organizational and institutional proportions.

CONCLUSION

The process of implementing industrial structural modernization unfolds through several key stages. In the initial stage, the objectives and goals of structural reforms are defined. The second stage involves assessing the competitiveness of industrial sectors and evaluating the technological maturity of industrial production. In the third stage, a forward-looking strategy is formulated, and the restructuring of industrial enterprises is executed. Finally, in the fourth stage, conclusions are drawn, and the effectiveness of the modernization measures is assessed.

REFERENCES

1 «Industrija 4.0»: sozdanie cifrovogo predprijatija. «Vsemirnyj obzor realizacii koncepcii “Industrija 4.0” v promyshlennyh kompanijah za 2016 god». [Jelektronnyj resurs]. URL: https://www.pwc.ru/ru/technology/assets/global_industry-2016_rus.pdf

2 Promyshlennost' Respubliki Kazahstan / ctatisticheskij sbornik / na russkom jazyke / 194 s. Astana. 2024

3 Lobanov M.M. Strukturnaja modernizacija promyshlennosti stran CVE /V sbornike: Jekonomika dlja cheloveka: social'no-orientirovannoe razvitie na osnove progressa real'nogo

sektora // Materialy Moskovskogo jekonomicheskogo foruma / Pod red. R.S. Grinberga, K.A. Babkina, A.V.Buzgalina. - 2014. - S. 739-743.
4 Tenjakov I.M. Teoreticheskie i prakticheskie problemy vosproizvodstva obshhestvennogo kapitala, jekonomicheskogo rosta i strukturnoj modernizacii promyshlennosti // Vestnik Moskovskogo universiteta. Serija 6: Jekonomika. - 2011. - №2. - S.110-120.
5 Rodrik D. Normalizing Industrial Policy //Working Paper of the Commission on Growth and Development of the World Bank. - 2008. - N 3. - P. 1 - 36.
6 Altenburg T. Industrial Policy in Developing Countries // Discussion Paper of the German Development Institute. - 2011. - N 4. - P. 1 - 97.
7 Bat'kovskij M.A., Kravchuk P.V. Modernizacija i strukturnaja perestrojka innovaciono-aktivnyh predprijatij naukoemkih otraslej promyshlennosti // Rostovskij nauchnyj zhurnal. - 2019. - № 1. - S. 111-122.
8 Chebanov A.A. Conceptual basis of industrial structure modernization // Biznes inform. - 2012. N 11. - C.134-137.

IRSTI 28.19

ROBOT VISION: CONCEPT AND CAPABILITIES

Izturganov N.D., Musabekov A.A.*, Baigabylova D.K., Akhmetova K.T., Markabaeva D.B.
M.Auezov South Kazakhstan University, Shymkent, Kazakhstan
***Corresponding Author's Email:** berik.mirza@mail.ru*

ABSTRACT

An introduction to robot vision technologies reveals one of the most exciting aspects of modern robotics. Vision systems for robots allow machines to "see" and analyze the surrounding world, which is key to creating more autonomous and intelligent robots. Using special cameras, sensors, and complex image processing algorithms, robots can now recognize objects, estimate distances, differentiate shapes and colors, and even react to dynamic changes in the environment. Robotic vision goes beyond simple image capture. It encompasses many aspects, from image filtering and segmentation to deep learning and pattern recognition, enabling the system to adapt to varying lighting conditions and tasks. With libraries like OpenCV and TensorFlow, and robotics platforms such as ROS, engineers can develop flexible and customizable solutions for object recognition, spatial orientation, and automated control.

Keywords: OpenCV, robotics, Machine Vision, Monochrome Vision, TensorFlow, ROS, intelligent systems.

INTRODUCTION

Types of Robot Vision and Software Examples

Today, robotic vision is widely used in various fields, including industrial manufacturing, logistics, medicine, and transportation. It plays a crucial role in the development of autonomous vehicles, medical robots, industrial manipulators, and security systems. As machine vision technologies continue to advance, robotic systems will become even more accurate, efficient, and, importantly, safer for working in the world around us.

Robot vision is an area of robotics and artificial intelligence that focuses on giving machines the ability to perceive the surrounding world and interpret visual information. This is achieved through cameras, sensors, and complex image processing algorithms. Robotic vision allows robots to navigate space, recognize objects, and perform tasks that require "vision." It is a combination of hardware and software that enables robots to "see," interpret, and respond to visual information in real time. For this, robots use cameras and sensors, and their "vision" is implemented through image processing algorithms and machine learning.

Types of Robot Vision and Software Examples

1. Monochrome Vision

In monochrome systems, images are transmitted and processed in shades of gray, saving computational resources. Algorithms based on OpenCV, a popular computer vision library, are often used to analyze the shape, contours, and texture of objects. An example of this is in industrial quality control, where monochrome cameras analyze the shape of parts to detect defects.

2. Color Vision

In this type of vision, the robot perceives the full color spectrum, allowing it to analyze objects by color. Systems use libraries like OpenCV, TensorFlow, or Keras for object classification and recognition.

Example: Robots on sorting lines that distinguish and sort objects by color. Programs based on color segmentation algorithms enable the robot to recognize objects and sort them, for instance, using an artificial neural network for color classification.

3. Stereoscopic Vision

By using two cameras, the robot can determine the distance to objects and create simple 3D models of the environment. Libraries like ROS (Robot Operating System) integrate stereoscopic vision for navigation and object manipulation. A key element of stereoscopic vision software is image matching algorithms, such as SIFT and ORB, which help cameras "understand" depth and spatial relationships between objects.

4. 3D Vision (LiDAR)

LiDAR technology uses lasers to create detailed 3D maps of the environment. LiDAR vision software often includes libraries such as PCL (Point Cloud Library), which processes and visualizes three-dimensional data. Algorithms in PCL allow the creation of accurate 3D models of space, crucial for autonomous robots and vehicles. For example, a Tesla car uses complex models that integrate LiDAR data with camera data to understand the position and distance to objects on the road.

5. Thermal Vision

In this system, robots are equipped with infrared cameras, enabling them to distinguish heat sources. Programs based on OpenCV and MATLAB can analyze thermal images, highlighting the thermal contours of objects. For instance, drones equipped with thermal vision use segmentation and filtering algorithms to detect thermal signals, which is especially useful in low visibility conditions or for search-and-rescue missions.

6. Machine Vision with Deep Learning

These are complex systems that learn to recognize and classify objects based on neural networks. Libraries such as TensorFlow and PyTorch allow the creation and training of deep neural networks for analyzing complex visual scenes. Deep learning machine vision programs often use models like CNN (Convolutional Neural Networks) and R-CNN (Regional Convolutional Networks), enabling the recognition of faces, animals, vehicles, and other complex objects. Example: Robots like Pepper, which analyze the environment and interact with people using facial and object recognition.

Examples of Software for Implementing Robotic Vision

- OpenCV (Open Source Computer Vision Library): A library suitable for image processing, segmentation, contour, and shape recognition. It is used in various robots to implement basic vision functions.

- TensorFlow and Keras: Libraries for deep learning used for object classification and pattern recognition. These are applied in robots requiring the analysis of complex visual data, such as autonomous vehicles.
- ROS (Robot Operating System): A specialized platform for developing software for robots, including modules for processing data from cameras and sensors, stereoscopic and 3D vision. It is popular in research and industrial robotics.
- PCL (Point Cloud Library): Used for working with point clouds generated by 3D sensors such as LiDAR. It is applied in autonomous vehicles and industrial robots for spatial orientation.
- YOLO (You Only Look Once): An algorithm for fast real-time object recognition. It allows robots to identify objects and actions, useful in various scenarios, from industrial sorting to security applications.

Examples of Robots with Various Types of Vision

- Amazon Robotics: In Amazon's warehouse robots, color and stereoscopic vision are used to differentiate and capture objects.
- Boston Dynamics (Spot): A robot with 3D vision and LiDAR, used for research and industrial purposes.
- Tesla Cars: Utilize 3D vision and machine learning for autonomous driving.
- iRobot Cleaning Robots: Use machine vision to recognize obstacles and plan their cleaning routes.

Robotic vision continues to develop and becomes increasingly sophisticated, enabling robots to perform complex tasks that were once considered exclusively human abilities.

MATERIALS AND METHODS

Hardware Components. The robot vision system was developed using a combination of hardware and software components. The primary hardware includes: Camera Module: A high-resolution RGB-D camera (Intel RealSense D435) for capturing depth and color images. Processing Unit: NVIDIA Jetson Xavier NX for real-time image processing and deep learning inference. Sensors: Additional LiDAR (Velodyne VLP-16) for enhanced spatial awareness. Actuation System: Servo-controlled pan-tilt mechanism for dynamic field-of-view adjustments.

Software Framework. The robot vision system was implemented using an integrated software stack composed of: Operating System: Ubuntu 20.04 with ROS2 (Robot Operating System) for seamless integration of components. Computer Vision Libraries: OpenCV and PCL (Point Cloud Library) for image processing and point cloud manipulation. Deep Learning Models: Pre-trained convolutional neural networks (CNNs) such as YOLOv5 and Faster R-CNN for object detection. SLAM Algorithm: ORB-SLAM3 for real-time localization and mapping.

Data Acquisition and Processing. The system captures and processes data using the following workflow: Image Capture: The RGB-D camera records frames at 30 FPS, providing depth and color images. Preprocessing: Image normalization, noise reduction, and edge enhancement techniques are applied. Feature Extraction: Keypoints and descriptors are extracted using SIFT (Scale-Invariant Feature Transform). Object Recognition: CNN-based models classify and detect objects in real time. Mapping and Localization: Depth data is processed using SLAM algorithms to generate a 3D representation of the environment. Decision Making: Based on object recognition and spatial awareness, the system plans and executes robotic movements.

Performance Evaluation. The system was evaluated under controlled conditions with the following parameters: Accuracy of Object Detection: Measured using precision, recall, and F1-score. Processing Latency: Evaluated in milliseconds per frame. Robustness to Environmental Variations: Tested under different lighting and occlusion scenarios.

Experimental Setup. Experiments were conducted in a controlled lab environment as well as in an unstructured outdoor setting to assess real-world performance. The test environment included various objects of interest, obstacles, and dynamic elements to evaluate adaptability.

This methodology ensures a comprehensive assessment of the robot vision system’s capabilities and performance in diverse operational scenarios.

RESULTS AND DISCUSSION

The robot vision system was evaluated based on several performance metrics, including object detection accuracy, processing speed, and adaptability to environmental variations. The key findings are as follows:

Object Detection Accuracy: The system achieved an average precision of 92.5% and recall of 89.8% in controlled conditions. Under real-world environments, performance slightly declined to 87.3% precision and 85.2% recall due to varying lighting and occlusions.

Processing Latency: The processing speed was measured at an average of 45 milliseconds per frame, enabling real-time execution with minimal delay.

SLAM Performance: The ORB-SLAM3 algorithm effectively constructed a 3D map with an average localization error of 3.2 cm in controlled conditions and 5.7 cm in unstructured environments.

The obtained results highlight the efficiency and robustness of the proposed robot vision system. Several observations were made during the evaluation:

Accuracy vs. Environmental Factors: While the system performed well in controlled conditions, external factors such as poor lighting and dynamic obstacles led to minor accuracy reductions. Enhancements such as adaptive exposure correction and improved occlusion handling could mitigate these effects.

Real-time Performance: The system's low latency processing confirms its suitability for real-time applications. Optimization through model pruning and hardware acceleration could further enhance speed and efficiency.

Robustness of SLAM: Despite minor errors, the mapping and localization capabilities demonstrated high reliability, making the system suitable for autonomous navigation in diverse environments.

Future Improvements: Additional training on a more diverse dataset, incorporation of multi-modal sensor fusion, and implementation of advanced deep learning models could further improve performance and adaptability.

The findings confirm the viability of the robot vision system for real-world applications, including industrial automation, autonomous navigation, and human-robot interaction. Future research should focus on enhancing robustness and adaptability to further refine its practical implementation.

CONCLUSION

The conclusion about robot vision systems highlights that this is one of the most advanced and in-demand technologies in robotics. It allows robots to "see" and interact effectively with the physical world, a capability that was once exclusive to humans. With the development of image processing techniques, machine learning, and artificial intelligence, robots can interpret visual data, detect and classify objects, and respond to changes in the environment in real time.

Modern robot vision systems have been made possible by advances in image processing and machine learning. Today, robots not only "see" but also understand visual information, enabling their use in a wide range of industries— from healthcare and manufacturing to home and public services.

Robotic vision is applied in various fields: from manufacturing automation and sorting to autonomous driving and security systems. Systems based on OpenCV, TensorFlow, ROS, and other specialized libraries allow the creation of diverse solutions for robotics, enhancing the accuracy and flexibility of robots' interaction with the world. Key areas of development include improving image processing in real-world conditions, adapting to changing lighting levels, expanding capabilities for stereoscopic and 3D vision, and integrating with other sensors to create comprehensive spatial perception. In the future, robotic vision technologies are expected to become even more powerful and ubiquitous, facilitating the creation of intelligent systems capable of perceiving and understanding the world just like humans.

REFERENCES

1 Kerr D.R. analysis, Propertie sand Designofa Stewart Platform Transducer // Trans. ASME. Journal Mechanisms, Transmissions and Automationin Design. 2018.No1.P.25-28.

2 K. Makino, H. Terada, VISUALISATION APPROACH FOR PREDICTION AND ANALYSIS OF EFFICIENCY OF AN OIL PUMP BASED ON GEOMETRICAL ARRANGEMENT, International Journal of Mechanics and Control, (Vol. 24, No. 1) pp. 97-106, 2023.

3 K. Berns and D. Görges, Preface for the Special Issue of the International Journal of Mechanics and Control (JoMaC) dedicated to 28th International Conference on Robotics in Alpe-Adria-Danube Region (RAAD 2019), International Journal of Mechanics and Control, Vol. 21, No. 01, p. 1, 2020.

4 M. Oehler, S. Kohlbrecher and O. von Stryk, Optimization-Based Planning for Autonomous Traversal of Obstacles with Mobile Ground Robots, International Journal of Mechanics and Control, Vol. 21, No. 01, pp. 33-40, 2020.

5 L. Scalera, A. Giusti, V. Di Cosmo, M. Riedl, R. Vidoni and D.T. Matt, Application of Dynamically Scaled Safety Zones Based on the ISO/TS 15066:2016 for Collaborative Robotics, International Journal of Mechanics and Control, Vol. 21, No. 01, pp. 41-50, 2020.

6 Ben-Hasan A., Daliri M. Arabian/Persian Gulf artisanal fisheries: magnitude, threats, and opportunities, Rev. Fish Biol. Fish. (2022), pp. 1-19.

7 Andrew J., Baker M., The general data protection regulation in the age of surveillance capitalism, Journal of Business Ethics, 168 (3) (2021), pp. 565-578.

8 Löhle S., Zander F., Eberhart M., Hermann T., Meindl A., Massuti-Ballester B., Leiser D., Hufgard F., Pagan A.S., Herdrich G., Fasoulas S.,Assessment of high enthalpy flow conditions for re-entry aerothermodynamics in the plasma wind tunnel facilities at IRS, CEAS Space J., 14 (2022), pp. 395-406.

INDUSTRIAL TECHNOLOGY AND ENGINEERING

Technical editor: *Nazarbek U.*

Signed for print on 12.09.2024

Format 70x100 1/16. Offset paper

Accounting-publishing list

Circulation 300 copies

CONTENTS

ISSN 2223-3911
03
9 772223 391166